

1 **Response to Reviewers**

2 We thank the reviewers for their constructive and helpful suggestions. We have
3 provided our responses to the reviewers' comments and believe that our manuscript is much
4 improved as a result.

5 The main paper improvements are:

- 6 • The abstract was rewritten.
- 7 • The goal of the study is formulated more clearly.
- 8 • The number of sites for validation of GELCA is increased.
- 9 • Proofreading and grammar check performed.

10 We added one more author Angel J. Gomez-Pelaez. The justification for additional author
11 is follows:

- 12 1. Angel J. Gomez-Pelaez is a data provider from the Izana WDCGG sites.
- 13 2. The contribution of additional author except of data providing includes also discussion of
14 the paper and revising of the manuscript.

15

16 The reviewer's specific comments (shown in blue) are addressed below.

1 **1. Response to Anonymous Referee #1**

2 Received and published: 8 September 2015#1:

3 The manuscript by Belikov et al. presents the development of a new adjoint modeling system
4 A-GELCA. The novelty of this tool is combining a Lagrangian back trajectory model with an
5 Eulerian adjoint model. The authors provide background on issues related to inverse
6 modeling of CO₂, which seems to be the intended application of this tool. The model estimates
7 for various configurations (different resolutions of the Eulerian component) are shown
8 compared to CO₂ measurements from seven stations in Siberia. This is followed by evaluation
9 of the model via comparison to forward modeling sensitivities and the Lagrange equality.
10 Lastly, the authors show comparisons of adjoint sensitivities for different model
11 configurations, highlighting the information brought through the coupling of Lagrangian and
12 Eulerian components. The tools presented here seem to perform adequately and will be of
13 value for future application studies. My main criticism is a lack of detail in many places in the
14 manuscript, particularly when covering some of the more essential and novel aspects of the
15 model development (how the Eulerian and Lagrangian components were coupled, or how the
16 adjoint code was developed). Further, the article needs much work on the grammar and
17 writing. I believe it will be suitable for publication after addressing these and other issues
18 outlined below.

19 Comments:

20 Scope: It seems like evaluation of the forward model is a substantial part of this work; as such,
21 this should be included in the abstract and introduction as one of the aims of the article, and
22 the title itself should reflect this scope.

23 The goal of this study is to present the development and evaluation of an Adjoint of the
24 Global Eulerian–Lagrangian Coupled Atmospheric model (A-GELCA). Evaluation of the
25 forward model is necessary to show the potential of the proposed method.

26
27 Abstract and throughout: it seems odd to refer to “development of the adjoint of a Lagrangian
28 model”, since Lagrangian models are self adjoint by construction. So saying “Lagrangian
29 adjoint” seems redundant.

30 Text in the paper was revised. “Lagrangian adjoint” is replaced with “Lagrangian
31 component”

32
33 5984.17: this entire sentence is rather vague. Could the authors clarify, quantitatively, what is
34 mean by “effective in reproducing”, “high uncertainty” and “low resolution”? Without any
35 numbers, such statements have little context or impact.

1 The sentence revised as follows: “The forward simulation shows that the coupled model
2 improves reproducing of the seasonal cycle and short-term variability of CO₂.”

3 However, we do not consider it is necessary to include any numbers in the introduction.
4 More details were added to main part.

5
6 5985.13: Can the authors be any more specific than “a number of studies have proposed
7 improvements” and then citing several papers? What are the improvements, and which are
8 relevant to the topic of this work in terms of those related to resolution, or coupled
9 Eulerian/Lagrangian frameworks?

10 Revised as follows:

11 “A number of studies have proposed improvements to the inverse methods of
12 atmospheric transport, i.e. the efficient computation of the transport matrix by the model
13 adjoint proposed by Kaminski et al. (1999b), use of monthly mean GLOBALVIEW-CO₂ ground-
14 based data (current version is for 2014) by Rödenbeck et al. (2003), development an
15 ensemble data assimilation method by Peters et al. (2005), flux inversion at high temporal
16 (daily) and spatial (model grid) resolution using for the first time of continuous CO₂
17 measurements over Europe by Peylin et al. (2005), use satellite data to constrain the
18 inversion of CO₂ by Chevallier et al. (2005), develop of a new observational screening
19 technique by Maki et al. (2010).”

20 Paper by Kaminski et al. (1999b) is related to the adjoint. Paper by Chevallier et al.
21 (2005) is related to use of satellite data. Flux inversion at high temporal (daily) and spatial
22 (model grid) resolution using for the first time of continuous CO₂ measurements over Europe
23 is discussed by Peylin et al. (2005).

24 Eulerian/Lagrangian frameworks is discussed later (5987.10-16): “In order to exploit
25 the advantages of both methods, Lagrangian and Eulerian chemical transport models can be
26 coupled to develop an adjoint, that is suitable for the simultaneous estimation of global and
27 regional emissions. Coupling can be performed in several ways; e.g., a regional-scale LPDM
28 can be coupled to a global Eulerian model at the domain boundary (Rödenbeck et al., 2009;
29 Rigby et al., 2011), or a global-scale LPDM can be coupled to an Eulerian model at the time
30 boundary (Koyama et al., 2011; Thompson and Stohl, 2014).”

31
32 5985.20: For recent measurement updates, a reference from 1999 doesn't seem very recent.

33 Replaced with (Karion et al., 2013; Tohjima et al., 2015)

1

2 5986.16: It would take a prohibitively large number of forward model evaluations to evaluate
3 such a matrix for an inversion with the same resolution of an adjoint-based approach.

4 Revised as: “Theoretically, to compute such matrix the transport model is run multiple
5 times with set of prescribed surface fluxes. However, this would require an extremely large
6 number of forward model evaluations. The adjoint of the transport model is an efficient way
7 to accelerate calculation of concentration gradient of the simulated tracer at observational
8 locations (Kaminski et al., 1999).”

9

10 5986.24: “Recent studies. . .” It seems odd to switch the discussion here to CO, given the
11 previous focus on long-lived tracers, CO₂ in particular. Why not instead cite/discuss the set of
12 current studies using adjoint models to invert satellite CO₂ data? I believe there are several.

13 Revised as follows: “Recent studies have used this method to constrain estimates of the
14 emissions of CO₂ using retrieved column integrals from the GOSAT satellite (Basu et al., 2013;
15 Deng et al., 2014; Liu et al., 2015).”

16

17 5986.28: “. . .speeds the process of inverse modeling” is only true for high dimensional
18 systems.

19 In 5985.23-30 we stated: “The satellite observation data from current (GOSAT, Kuze et
20 al., 2009; Yokota et al., 2009; OCO-2, Crisp et al., 2004) and future missions
21 (CarbonSat/CarbonSat Constellation; Bovensmann et al., 2010; Buchwitz et al., 2013) offer
22 enormous potential for CO₂ inverse modeling. Optimal application of large observed datasets
23 requires expanding the inverse analysis of CO₂ to finer resolution, higher precision and faster
24 performance.” A large number of observations and resolution of the considered model
25 indicate that the existing and developing inverse modeling system can be attributed to the
26 high dimensional systems.

27

28 5988.20: The background. . .” I didn’t really understand what was being said here or how the
29 modeling setup works in this regards.

30 Here “The background grid values of the concentrations” are the concentrations
31 calculated by Eulerian model.

32 To clarify the sentences about the model setup we revised section 2.1.

1

2 5989.3: The description of the coupling of the eulerian adjoint model with the Lagrangian
3 model is rather vague. This statement, that it was coupled at the “time boundary” is made a
4 few times, but to be honest I don’t really know what it means. Given that (a) this coupling is
5 the single most unique and exciting feature of the A-GELCA model and (b) articles in GMD are
6 for the expressed purpose of describing algorithmic model details, this should be clarified in
7 further detail, at the level of making the process understandable and reproducible by a reader.

8 We revised section 2.1 and added short descriptions of coupling procedure to the text to
9 clarify the sentences about the time boundary coupling: “The scheme of concentration
10 calculation for the given location includes coupling of two model approaches. NIES TM
11 calculates global concentrations for the selected time period (usually 1 year to exclude spin-
12 up effect), but stops 7 days before the time of the observations. To obtain the concentrations
13 for the observation time we transport the background concentrations from NIES TM gridbox
14 to the location of observation point along the trajectory ensemble calculated by FLEXPART
15 model and add contribution from surface sources. Therefore we have implemented the
16 coupling at a time boundary in the global domain of the NIES transport model, while nested
17 regional modeling systems such as one by Rodenbeck et al (2009) have to couple at both
18 region boundary and time boundary.”

19 Here we just repeat the main features of the coupling. Detailed information may be
20 found in original paper by Ganshin et al. (2012).

21

22 5989.25: “performs well” is very vague. Can the authors be more specific?

23 The text is revised as follows: “To ensure that this is the case, the NIES TM model has
24 been evaluated extensively. Comparisons against SF₆ and CO₂ (Belikov et al., 2011, 2013b),
25 CH₄ (Patra et al., 2011; Belikov et al., 2013b), and ²²²Rn (Belikov et al., 2013a) measurements
26 show the model ability to reproduce seasonal variations, interhemispheric gradient and
27 vertical profiles of tracers.” For details please check papers shown above.

28

29 5992.5: Is it that the errors are unbiased or that the background estimate itself is unbiased?

30 Here it is assumed, the model simulations are unbiased. Observations are unbiased
31 normally.

32

1 5992.6: This capital bold H applied as a matrix is already linear by definition. If the authors
2 intended to more generally describe a potentially nonlinear forward model operator, they
3 should use capital cursive H.

4 Revised as follows: “The minimization of the cost function (Eq. 2) has an analytic
5 solution ...”

6 Did the authors also generate/evaluate a tangent linear model? If not, what is there intended
7 path towards deriving an inverse modeling system (many formulations of which require a
8 tangent linear model, i.e., incremental 4D-Var with CG optimization, etc)? Or will their system
9 only worth with optimization approaches such as using the BFGS variable-metric quasi-
10 newton algorithm?

11 Yes, we constructed tangent linear model. We stated “The tangent linear and adjoint
12 components of the Eulerian model ...” at 5984.7, 5994.1, 5999.22.

13

14 5993.11: Previously (5992.24) a 1x1 scale was referred to as low resolution, but here 1x1 is
15 used for the “high resolution” FLEXPART runs. This is a bit inconsistent. I was expecting
16 FLEXPART simulations to be run at a much finer (i.e. 10’s of km) scale.

17 At line 5992.24 the sentence “standard low-resolution” replaced with “standard
18 resolution”.

19 Currently we have no meteorological data suitable to run the FLEXPART model with
20 higher resolution (i.e. 0.5 degree). However, use a model with resolution of 1x1 degree for flux
21 inversion is normal now.

22

23 The set of measurements used for evaluation (7 sites) seems pretty thin compared to the
24 amount of available CO2 measurements available. The NOAA GMD network alone has more
25 than 100 measurement sites. Now, perhaps forward model evaluation isn’t a goal of this work
26 (see previous discussion, this wasn’t clear), but if it is then it should be done more
27 comprehensively.

28 Number of sites for validation of GELCA is increased. Section 4 was revised.

29

30 5994.7: “We recognize. . . is quite problematic” I didn’t understand the point that the authors
31 are trying to make here. Can they reword?

32 Reworded: “We recognize that is quite problematic to use the highly uncertain surface
33 fluxes to simulate the tracer concentrations and use these concentrations for estimating the
34 quality of different model configurations. Nevertheless, we cannot improve our analysis,
35 because we do not have concentration measurements for tracers whose surface fluxes are

1 more accurately known, like SF6.”

2

3 5994.22: I recognize that there are continuous vs discrete approaches for developing adjoint
4 models, that there are benefits/drawbacks to each approach, and that the authors have
5 adopted the discrete approach for specific reasons. But is it fair to only here mention the
6 benefits of this approach, and none of the drawbacks?

7 We added “The main drawback of the method is that the deriving of discrete adjoint of
8 Eulerian model is a significant technical challenge.”

9

10 5996: For the forward model sensitivity, use λ_F throughout, not just in equation 5.

11 Revised accordantly.

12

13 5996.14: Why is a perturbation needed for an adjoint simulation? Do you mean forcing? Or
14 that the cost function was defined to be 1 ppm per grid cell?

15 There was misprint in this section.

16 The text was revised, as: “In the first test, adjoint simulations were carried out using an
17 initial CO₂ distribution, zero surface flux for 2 days (1-2 January 2010) and a horizontal grid
18 with resolution 2.5° × 2.5°. The adjoint gradient was then compared with that from the finite
19 difference calculated using Eq. (3). This equation was selected in order to save CPU time by
20 minimizing the number of forward model function calculations. For this test we used $\varepsilon = 0.01$.”

21

22 Section 3: I recognize that the long-term goal is inverse modeling. However, the application
23 and testing of the model thus far is just for sensitivity calculations. It seems then that Section 3
24 would be better served as a description of adjoint modeling, and the background of how this
25 works, rather than or in addition to inverse modeling, as the latter isn’t actually done in the
26 present manuscript. This would help clarify, for example, the setup of the adjoint calculations
27 that are performed later for validation in 5.2.1, which I don’t believe used a cost function of
28 the type shown here, but rather something different.

29 Section 3 is necessary to show why the adjoint has been developed and attach
30 consistency to the article. A simplified form of the described cost function is used to validate
31 the adjoint.

32

1 5996.15: The forward sensitivity calculation was performed in how many locations? It seems
2 from Fig 3 that they were done in many grid cells, in order to compare to the adjoint results
3 throughout the domain of this figure, but that would be very expensive, computationally, even
4 using Eq 3. If transport was turned off for the testing, all locations could have been tested
5 simultaneously, but this wouldn't constitute a very meaningful test of the adjoint of the tracer
6 transport model.

7 The forward sensitivity calculation was performed using Eq 3 at the same grid cells as
8 for the adjoint simulation. Indeed it is very expensive, computationally. However, this is very
9 powerful test, as it make possible to compare to the adjoint results throughout the domain.

10

11 5.2.1: What was the state vector used for these tests? CO₂ initial conditions? Fluxes? Or flux
12 scaling factors? What are the corresponding units of the results shown in Fig 3?

13 The state vector is flux, the target value is concentration. CO₂ initial conditions and
14 fluxes are same as for the GELCA forward simulations (added to text). The units
15 (ppm/($\mu\text{mol}/\text{m}^2\text{s}$)) are added to the figure caption.

16

17 5997.10: It would probably be good to show results from these tests somehow.

18 We revised text as follows: "We use Eq. (7) to test the adjoint model initialized using
19 several different random random vectors \mathbf{u} and \mathbf{v} . For all cases, Eq. (7) compares well within
20 machine epsilon with mismatch between -3e^{-14} to 6e^{-14} ."

21

22 Figs 4-6: These are really interesting results. I found myself, however, having to flip back and
23 forth between these figures to compare across the different modeling approaches.

24 Comparison for a single method across days was much less interesting or relevant to this
25 work. So I would suggest reducing these figures to a single figure that shows the results for a
26 single day but for the 4 methods: eulerian, Lagrangian (native), Lagrangian (aggregated),
27 coupled.

28 We tried to make the figures easier to compare and combine them appropriately. Section
29 5.2.2 was revised.

30

31 5999: "substantial amount of manual programming effort is required" This should be
32 expanded for a GMD article.

33 We revised paragraph 5995.1-5 to add more detail about manual code developing, as
34 follows: "The tangent linear and adjoint models of the NIES TM to FLEXPART coupler were

1 derived using the automatic differentiation software TAF (<http://www.FastOpt.com>), which
2 significantly accelerated the development. However, considerable manual processing of
3 forward and adjoint model codes was necessary to improve the transparency and clarity of
4 the model and to optimize the computational performance of, including MPI, as the TAF code
5 used here (version 1.5) does not fully support MPI routines.”

6

7 Editorial:

8 This manuscript needs a thorough proofreading and grammar check prior to publication. I’ve
9 provided comments below on the abstract and introduction but stopped after that point.

10 5984.7 tangent -> tangent linear

11 Revised

12 5984.6: paragraph break not needed

13 Revised

14 5984.11: as results -> as a result

15 Revised

16 5984.11: of Eulerian -> of the Eulerian

17 Revised

18 5984.17: “test experiments” is redundant, suggest just “tests” or “experiments”.

19 Revised

20 5984.17: shown -> shows

21 Revised

22 abstract: the written tense keeps changing, please try to use a single tense throughout.

23 The abstract was rewritten.

24 5984.20: demonstrates the -> is (or was, depending on if you decide to write in the past or
25 present tense throughout) shows to have

26 5985.18: a density ->the density

27 Revised

28 5985.19: measurements -> more measurements

29 Revised

30 5985.21: global scale CO2 observation are not existing-> global scale in situ CO2 observations
31 do not exist

32 Revised

1 5986.10 CO2 a -> CO2, a
2 Revised

3 5986.12: If tracer is a chemically inert -> For chemically inert tracers,
4 Revised

5 5986.15: running multiple times with set -> run multiple times with different sets of
6 Revised

7 5986.19: Seems odd to have the paragraph break here, instead of e.g. line 22.
8 Revised

9 5986.29: “memory demands” should be minimal for adjoint approaches with inert tracer
10 transport (i.e. linear) models.
11 Indeed, the adjoint approach has relatively low CPU and memory demands. However,
12 here we pointed out computational cost of Eulerian chemical transport models (CTMs) with
13 the high-resolution grids in adjoint and forward simulations.
14

15 5987.1 “It would. . . fluxes” This sentence doesn’t make much sense, and needs to be rewritten.
16 Revised as follows: “It would be beneficial to increase the model resolution close to
17 observation points, where the strong observation constraint can significantly improve the
18 optimization of the resulting emission fluxes.”
19

20 5987.10: utilize of the -> utilize the
21 Revised

22 5987.11: the adjoint, which -> an adjoint that
23 Revised

24 5987.17: “One goal” is there another goal of this work? Forward model evaluation perhaps? If
25 so this other goal should also be directly stated. If not, suggest saying “The goal”.
26 Revised. “The goal of this study is ...”

27 Eq 1: why does the “l” index start at 0 and the others at 1?
28 “l” is a time index, while others are coordinates
29

1 **2. Response to Anonymous Referee #2**

2 Received and published: 8 September 2015

3 Overview:

4 The manuscript “Adjoint of the Global Eulerian–Lagrangian Coupled Atmospheric transport
5 model (A-GELCA v1.0): development and validation” by Belikov et al. describes the
6 construction of a new coupled adjoint model based on GELCA, which is a coupled forward
7 transport model based on the NIES Eulerian transport model and the Lagrangian transport
8 model, FLEXPART. The methodology described in this manuscript provides an interesting
9 development upon existing adjoint models, and may be used in future to supply high-
10 resolution adjoint sensitivities at relatively low computational cost. The authors describe the
11 applications of the model, before describing its development and providing examples of the
12 adjoint model’s accuracy in comparison with the forward model. Finally, a real-world example
13 of use of the adjoint model is described.

14 Overall the manuscript is fairly clearly written, although there are a large number of technical
15 corrections necessary before publication. Some of the descriptive sections are quite brief and
16 lacking in necessary detail. The figures and tables are generally clear and well chosen.

17 Although the performance of the forward coupled model compared with the Eulerian model is
18 investigated to some extent, my biggest concern with the manuscript is that only a handful of
19 sites are included in this analysis, all of which are in relatively close proximity to each other,
20 in a region where surface fluxes are uncertain. However, from this limited perspective, the
21 coupling does appear to improve the model performance. The adjoint model is shown
22 satisfactorily to be accurate in comparison with the forward model, which is the most
23 important aspect of the manuscript.

24 I recommend publication after these revisions have been carried out.

25 Comments:

26 5985.11: define 3-D for first use

27 Done

28 5985.20: Can you provide a more recent reference than Bovensmann et al., (1999) for this
29 statement?

30 Replaced with (Karion et al., 2013; Tohjima et al., 2015)

31 2986.2-4: Rephrase: “Generally, there are the Eulerian and the Lagrangian method of
32 modelling the atmospheric constituents transport”

33 Rewritten as “Generally, the atmospheric constituents transport may be described in
34 two different ways: the Lagrangian and the Eulerian approaches.”

1 5986.16: Rephrase the sentence beginning “The adjoint of the transport model. . .” as it is
2 unclear.

3 Revised as: “The adjoint of the transport model is an efficient way to accelerate
4 calculation of concentration gradient of the simulated tracer at observational locations
5 (Kaminski et al., 1999).”

6
7 5986.24: The accompanying references to this sentence seem out of place here, as they relate
8 to inverse modelling of CO and NO_x, rather than the longer-lived species discussed in the rest
9 of the manuscript.

10 Revised as follows: “Recent studies have used this method to constrain estimates of the
11 emissions of CO₂ using retrieved column integrals from the GOSAT satellite (Basu et al., 2013;
12 Deng et al., 2014; Liu et al., 2015).”

13

14 5987.3: You should mention recent work that has made use of nested grids together with
15 inverse modelling methods in order to obtain high-resolution inverse results, such as
16 Hooghiemstra et al., (2012).

17 Paper by Hooghiemstra et al., (2012) relates “to inverse modelling of CO, rather than the
18 longer-lived species discussed in the rest of the manuscript.” Please see previous comment.

19

20 5988.19: Have you investigated the effect of changing the number of particles used in the
21 Lagrangian model (both in terms of information content and computational time)? Perhaps
22 you should mention how you settled on 1000 particles.

23 Added: “The number of particles has been chosen to optimize the computational cost
24 without compromising the quality of modeling by Ganshin et al., (2013).”

25 More details are in paper by Ganshin et al., (2013): “One thousand particles were used in
26 the calculations with our method, and this number was found to be optimal by comparing
27 calculations using different numbers of particles. Increasing the number of particles by an
28 order of magnitude (up to 10000) improves the results slightly but increases the required
29 computer time many times. On the other hand, decreasing the number of particles to below
30 100 markedly worsens model data.”

31

1 5989.3: You should clarify what it means to have a coupling at the time boundary in the global
2 domain, rather than at the spatial boundaries. I felt that this was unclear, and should be
3 clearly explained in a development manuscript such as this one.

4 We revised section 2.1 and added short descriptions of coupling procedure to the text to
5 clarify the sentences about the time boundary coupling: “The scheme of concentration
6 calculation for the given location includes coupling of two model approaches. NIES TM
7 calculates global concentrations for the selected time period (usually 1 year to exclude spin-
8 up effect), but stops 7 days before the time of the observations. To obtain the concentrations
9 for the observation time we transport the background concentrations from NIES TM gridbox
10 to the location of observation point along the trajectory ensemble calculated by FLEXPART
11 model and add contribution from surface sources. Therefore we have implemented the
12 coupling at a time boundary in the global domain of the NIES transport model, while nested
13 regional modeling systems such as one by Rodenbeck et al (2009) have to couple at both
14 region boundary and time boundary.”

15 Detailed information may be found in original paper by Ganshin et al. (2012).

16
17 5989.25: You say that the model performs well in comparison with measurements, but you
18 should further clarify this statement. Can you quantify the performance? Are there any major
19 discrepancies in the model performance in (e.g.) interhemispheric exchange time or vertical
20 mixing?

21 The text is revised as follows: “To ensure that this is the case, the NIES TM model has
22 been evaluated extensively. Comparisons against SF₆ and CO₂ (Belikov et al., 2011, 2013b),
23 CH₄ (Patra et al., 2011; Belikov et al., 2013b), and ²²²Rn (Belikov et al., 2013a) measurements
24 show the model ability to reproduce seasonal variations, interhemispheric gradient and
25 vertical profiles of tracers.” More details are in papers shown above.

26
27 5992.6: H is, by definition, already linear if it is a matrix.

28 Revised as follows: “The minimization of the cost function (Eq. 2) has an analytic
29 solution ...”

30
31 5993.27-29: I do not think that this statement is supported by the values provided in Table 3.
32 The high-resolution Eulerian model variously outperforms and is outperformed by the low-
33 resolution coupled model at different sites. You should either remove or add qualifications to
34 this line.

1 Section 4 was revised entirely.

2
3 5994.10: Although you have mentioned this in the text, I'm bothered by the fact that you have
4 assessed the model performance at only a few sites in one region of the globe. There exist a
5 number of observational datasets available for comparisons to model data, such as those
6 provided by the Global Monitoring Division of the National Oceanic and Atmospheric
7 Administration. Can you examine the coupled model performance in tropical regions, for
8 example?

9 Number of sites for validation of GELCA is increased. Section 4 was revised.

10

11 5996.12: This explanation of the model set-up for the accuracy test is a little unclear and
12 should go into more detail. What do you mean by "perturbed by 1ppm per grid cell"?

13 There was misprint in this section.

14 The text was revised, as: "In the first test, adjoint simulations were carried out using an
15 initial CO₂ distribution, zero surface flux for 2 days (1-2 January 2010) and a horizontal grid
16 with resolution 2.5° × 2.5°. The adjoint gradient was then compared with that from the finite
17 difference calculated using Eq. (3). This equation was selected in order to save CPU time by
18 minimizing the number of forward model function calculations. For this test we used $\varepsilon = 0.01$."

19

20 5996.15: The sentence is unclear and needs rephrasing. How exactly are you saving CPU time
21 here?

22 The sentence was revised as follows: "The adjoint gradient was then compared with that
23 from the finite difference calculated using Eq. (3). This equation was selected in order to save
24 CPU time by minimizing the number of forward model function calculations. For this test we
25 used $\varepsilon = 0.01$."

26 In Eq. (3) evaluates perturbations at point $(\mathbf{x} + \varepsilon \cdot \mathbf{x}_e)$. Eq. (4) evaluates perturbations at
27 points $(\mathbf{x} + \varepsilon \cdot \mathbf{x}_e)$ and $(\mathbf{x} - \varepsilon \cdot \mathbf{x}_e)$. Thus, Eq. (4) requires a two times more simulations with
28 forward model.

29

30 5997.17: This section needs more explanation. What simulations did you carry out here,
31 exactly? What were your initial conditions for the adjoint model runs?

32 We added: "CO₂ initial conditions and fluxes were the same as those used for the CELGA
33 forward simulations in Section 4"

1 We revised the section entirely.

2
3 6013-14: Keep the same order of cases from left to right when printing R, M and S in the plots
4 (i.e. red-cs1, blue-cs2, green-cs3, not green, blue, red).

5 Done

6
7 Figures 4 – 7: It might be interesting to see panels showing the differences between the
8 different results when using the different versions of the model, as it can be difficult to discern
9 these differences by eye. Also, in Figure 5, are the left-hand and right-hand panels the same
10 results, but aggregated onto different grids? I can see the logic of this, but it feels a little
11 unnecessary to me to have both grids displayed. I'd consider showing only the results on the
12 native model grid, as Figure 6 shows the combined results on the 2.5 degree grid anyway.

13 It is difficult to show differences between the different results when using the different
14 versions of the model, because they have a different spatial extension. We tried to make the
15 figures easier to compare and combined them. The section revised.

16
17 Technical corrections: Overall, the manuscript requires a thorough proofreading in order to
18 make sure that there are no further technical corrections necessary. I have included all of the
19 mistakes that I found.

20 Done

21 5984.7: tangent -> tangent linear

22 Revised

23 5984.11: As results -> As a result

24 Revised

25 5984.17: shown -> shows that

26 Revised

27 5984.20: demonstrates the high accuracy -> demonstrates high accuracy

28 Revised

29 5985.18: a density of observational network -> the densityof the observational network

30 Revised

31 5985.21: CO2 observation are not existing -> CO2 observations do not exist

32 Revised

33 5986.13: If tracer is a chemically inert -> if a tracer is chemically inert

1 Revised

2 5986.15: is running -> is run

3 Revised

4 5986.28: speeds -> speeds up

5 Revised

6 5987.10: To utilize of the strongest sides of both methods -> In order to exploit the

7 advantages of both methods

8 Revised

9 5988.10: This may change in the font of the final manuscript, but the capital "I" and lower-

10 case "l" appear identical in this equation. Maybe consider changing notation?

11 Revised. "L" and "l" are replaced with "S" and "s" correspondently.

12 5989.12: The model's employs -> The model employs

13 Revised

14 5989.16: we follows -> we follow

15 Revised

16 5989.22: ration -> ratio

17 Revised

18 5989.25: intercomparisons -> comparisons

19 Revised

20 5990.2: FLEXPART similar to other LPDMs consider ... -> FLEXPART, like other LPDMs,

21 considers ...

22 Revised

23 5990.4: sink and sources -> sinks and sources

24 Revised

25 5990.5: running -> tracking? following?

26 Revised

27 5990.6: no comma necessary here

28 Revised

29 5990.11: Gaussian grid T106 -> Gaussian T106 grid

30 Revised

31 5990.12: and in 6h time steps -> and 6-hourly time steps.

32 Revised

- 1 5991.2: 3-dimensional -> 3D
2 Revised
- 3 5991.6: driving -> driven
4 Revised
- 5 5991.8: "The" current version
6 Revised
- 7 5991.10: Remove extra 'of'
8 Revised
- 9 5991.13: parameter estimation method used in different reanalysis dataset the use. . .
10 -> parameter estimation methods used in different reanalysis datasets, the use
11 Revised
- 12 5994.21: a construction of continuous adjoint -> construction of a continuous adjoint
13 Revised
- 14 5995.13: remoted -> remote (or distanced?)
15 Revised
- 16 5995.20: inpute -> input
17 Revised
- 18 5997.2: did not seriously changed -> did not significantly change
19 Revised
- 20 5997.8: the M in the denominator should be M' (i.e. tangent linear)
21 Revised
- 22 6000.12: Performed in the paper analyses showed, that GELCA -> Analyses in this paper
23 showed that GELCA. . .
24 Revised
- 25 6000.14: Decreasing of the Eulerian model resolution are not able to significantly distort. . . ->
26 Decreasing the Eulerian model resolution does not significantly distort. . .
27 Revised
- 28 6001.3: variation -> variational
29 Revised
- 30 6014: As Fig 2 -> As Fig 1
31 Revised
- 32 6015: Siberian observations towers -> Siberian observation towers

1 Revised

2 REFERENCES:

3 Hooghiemstra, P. B., M. C. Krol, T. T. van Leeuwen, G. R. van der Werf, P. C. Novelli, M. N.
4 Deeter, I. Aben, and T. Röckmann (2012), Interannual variability of carbon monoxide emission
5 estimates over South America from 2006 to 2010, *J. Geophys. Res.*, 117, D15308,
6 doi:10.1029/2012JD017758.

7

1 **Adjoint of the Global Eulerian–Lagrangian Coupled Atmospheric**
2 **transport model (A-GELCA v1.0): development and validation**

3 D.A. Belikov^{1,2,3}, S. Maksyutov¹, A. Yaremchuk⁴, A. Ganshin^{3,5}, T. Kaminski^{6,*}, S.
4 ~~Blessing~~⁶~~Blessing~~⁷, M. Sasakawa¹, Angel J. Gomez-Pelaez⁸ and A. Starchenko³

5 [1]{National Institute for Environmental Studies, Tsukuba, Japan}

6 [2]{National Institute of Polar Research, Tokyo, Japan}

7 [3]{Tomsk State University, Tomsk, Russia}

8 [4]{N. Andreev Acoustic Institute, Moscow, Russia}

9 [5]{Central Aerological Observatory, Dolgoprudny, Russia}

10 [6]{The Inversion Lab, Hamburg, Germany}

11 [~~7~~]{FastOpt GmbH, Hamburg, Germany}

12 ~~{*}~~~~now~~[8]{Izaña Atmospheric Research Center (IARC), Meteorological State Agency of Spain
13 (AEMET), Izaña, 38311, Spain}

14 ~~{*}~~~~Previously~~ at: ~~The Inversion Lab~~FastOpt GmbH, Hamburg, Germany}}

15

16 Correspondence to: D.A. Belikov (dmitry.belikov@nies.go.jp)

17

18

Abstract

We ~~present~~presented the development of the Adjoint of the Global Eulerian–Lagrangian Coupled Atmospheric (A-GELCA) model that consists of the National Institute for Environmental Studies (NIES) model as an Eulerian three-dimensional transport model (TM), and FLEXPART (FLEXible PARTicle dispersion model) as the Lagrangian ~~plume-diffusion model~~Particle Dispersion Model (LPDM).

The forward tangent linear and adjoint components of the Eulerian model were constructed directly from the original NIES TM code using an automatic differentiation tool known as TAF (Transformation of Algorithms in Fortran; <http://www.FastOpt.com>), with additional manual pre- and post-processing aimed at improving transparency and clarity of the code and optimizing the performance of the computing, including MPI (Message Passing Interface). ~~As results, the adjoint of Eulerian model is discrete. Construction of the adjoint of the~~The Lagrangian component did not require any code modification, as LPDMs are ~~able to self-adjoint and~~ track a significant number of particles ~~back~~backward in time ~~and thereby in order to~~ calculate the sensitivity of the observations to the neighboring ~~emission~~emission areas. ~~The constructed Eulerian and adjoint was coupled with the Lagrangian adjoint components were coupled component at the~~ time boundary in the global domain. ~~The results are verified~~ The simulations presented in this work were performed using a series of test experiments. the A-GELCA model in forward and adjoint modes. The forward simulation ~~shown~~shows that the coupled model ~~is effective in~~improves reproducing of the seasonal cycle and short-term variability of CO₂ ~~even in the case of multiple limiting factors, such as high uncertainty of fluxes and the low resolution.~~ The adjoint of the Eulerian model. ~~The adjoint model demonstrates the high accuracy was shown, through several numerical tests, to be very accurate~~ compared to direct forward sensitivity calculations ~~and fast performance~~. The developed adjoint of the coupled model combines the flux conservation and stability of an Eulerian discrete adjoint formulation with the flexibility, accuracy, and high resolution of a Lagrangian backward trajectory formulation. A-GELCA will be incorporated into a variational inversion system designed to optimize surface fluxes of greenhouse gases.

Keywords: atmospheric transport and inverse modeling, adjoint model, carbon cycle

3. Introduction

Forecasts of CO₂ levels in the atmosphere and predictions of future climate depend on our scientific understanding of the natural carbon cycle (IPCC, 2007; Peters et al., 2007). To estimate the spatial and temporal distribution of carbon sources and sinks, inverse methods are used to infer carbon fluxes from geographically sparse observations of the atmospheric CO₂ mixing ratio (Tans et al., 1989). The first comprehensive efforts in atmospheric CO₂ inversions date back to the late 1980s and early 1990s (Enting and Mansbridge, 1989; Tans et al., 1989). With the increase in spatial coverage of CO₂ observations and the development of ~~3D~~three-dimensional (3-D) tracer transport models, a variety of numerical experiments and projects have been performed by members of the so-called “TransCom” community of inverse modelers (e.g., Law et al., 1996, 2008; Denning et al., 1999; Gurney et al., 2002, 2004; Baker et al., 2006; Patra et al., 2011). A number of studies have proposed improvements to the inverse methods of atmospheric transport ~~(, i.e. the efficient computation of the transport matrix by the model adjoint proposed by Kaminski et al., (1999b;), use of monthly mean GLOBALVIEW-CO₂ ground-based data (current version is for 2014) by Rödenbeck et al., (2003;), development an ensemble data assimilation method by Peters et al., (2005;), flux inversion at high temporal (daily) and spatial (model grid) resolution using for the first time of continuous CO₂ measurements over Europe by Peylin et al., (2005;), use satellite data to constrain the inversion of CO₂ by Chevallier et al., (2005; Meirink et al., 2008;), develop of a new observational screening technique by Maki et al., (2010).~~ Despite progress in atmospheric CO₂ inversions, a recent intercomparison (Peylin et al., 2013) demonstrated the need for further refinement.

In recent decades, ~~athe~~ density of ~~the~~ observational network established to monitor greenhouse gases in the atmosphere has been increased, and ~~more~~ measurements taken onboard ships and aircraft are becoming available (~~BovensmannKarion et al., 1999-2013; Tohjima et al., 2015).~~ However, on a global scale CO₂ ~~observation are~~observations do not ~~existingexist~~ for many remote regions not covered by networks. This lack of data is one of the main limitations of atmospheric inversions, which can be filled by monitoring from space (Rayner and O’Brien, 2001). The satellite observation data from current (GOSAT, Kuze et al., 2009; Yokota et al., 2009; OCO-2, Crisp et al., 2004) and future missions (CarbonSat/CarbonSat Constellation; Bovensmann et al., 2010; Buchwitz et al., 2013) offer enormous potential for CO₂ inverse modeling. Optimal application of large observed datasets requires expanding the inverse analysis of CO₂ to finer resolution, higher precision and faster

1 performance.

2 To link surface fluxes of CO₂ to observed atmospheric concentrations, an accurate model
3 of atmospheric transport and an inverse modeling technique are needed. Generally, ~~there are~~
4 ~~the Eulerian and the Lagrangian method of modelling~~ the atmospheric constituents transport
5 may be described in two different ways: the Lagrangian and the Eulerian approaches. The
6 Eulerian method treats the atmospheric tracers as a continuum on a control volume basis, so
7 it is more effective ~~in~~ reproducing of long-term patterns, i.e. the seasonal cycle or the
8 interhemispheric gradient. The Lagrangian Particle Dispersion Models (LPDMs) consider
9 atmospheric tracers as a discrete phase and tracks each individual particle, therefore LPDMs
10 are better for resolving synoptic and hourly variations.

11 To relate fluxes and concentrations of ~~a~~ long-lived species like CO₂, a transport model
12 must cover a long simulation period (e.g., Bruhwiler et al., 2005). Therefore, computing time
13 is a critical issue and minimization of the computational cost is essential. ~~If tracer is a~~For
14 chemically inert tracers, the transport can be represented by a model's Jacobian matrix,
15 because the simulated concentration at observational sites is a linear function of the flux sets.
16 ~~To Theoretically, to~~ compute such ~~a~~ matrix ~~at~~ the transport model is ~~runningrun~~ multiple times
17 with set of prescribed surface fluxes. However, this would require an extremely large number
18 of forward model evaluations. The adjoint of the transport model is an efficient way to
19 ~~evaluate derivatives~~ accelerate calculation of concentration gradient of the simulated tracer at
20 observational locations ~~towards to the sources and sinks of tracer~~ (Kaminski et al., 1999).

21 Marchuk (1974) first applied the adjoint approach in atmospheric science. After that, this
22 method became widely used in meteorology. In the 1990s the use of this approach was
23 expanded to the field of tracer transport modeling (Elbern et al., 1997; Kaminski et al., 1999).

24 Adjoint models have numerous applications, including the data assimilation of
25 concentrations, inverse modeling of chemical source strengths, sensitivity analysis, and
26 parameter sensitivity estimation (Enting, 2002; Haines et al., 2014). Recent studies have used
27 this method to constrain estimates of the emissions of ~~various tracers~~CO₂ using retrieved
28 column integrals from the ~~GOME and MOPITT~~GOSAT satellite ~~instruments~~ (Müller and
29 ~~Stavrakou, 2005; Kopacz~~(Basu et al., ~~2009~~2013; Deng et al., 2014; Liu et al., 2015).

30 Using the adjoint model speeds up the process of inverse modeling. However, high CPU
31 and memory demands prevent us from using Eulerian chemical transport models (CTMs)
32 with high-resolution grids in inversions. It would be beneficial to increase the model
33 resolution close to observation points, where ~~small uncertainties in~~ the transport strong

1 | observation constraint can ~~seriously~~significantly improve ~~the~~ optimization of the resulting
2 | emission fluxes.

3 | LPDM running in the backward mode can explicitly estimate a source–receptor
4 | sensitivity matrix by solving the adjoint equations of atmospheric transport (Stohl et al.,
5 | 2009), which is mathematically presented by a Jacobian expressing the sensitivity of
6 | concentration at ~~the~~ observational locations. Marchuk (1995), and Hourdin and Talagrand
7 | (2006) ~~discussed the provided derivations proving~~ equivalence of the adjoint of forward
8 | transport models to backward transport models.

9 | ~~To utilize of~~In order to exploit the ~~strongest sides~~advantages of both methods,
10 | Lagrangian and Eulerian chemical transport models can be coupled to develop ~~the an~~ adjoint,
11 | ~~which that~~ is suitable for the simultaneous ~~estimation of~~simulation of contributions from
12 | global and regional emissions. Coupling can be performed in several ways; e.g., a regional-
13 | scale LPDM can be coupled to a global Eulerian model at ~~the a~~ regional domain boundary
14 | (Rödenbeck et al., 2009; Rigby et al., 2011), or a global-scale LPDM can be coupled to an
15 | Eulerian model at the time boundary (Koyama et al., 2011; Thompson and Stohl, 2014).

16 | ~~One~~The goal of this study is to present the development and evaluation of an Adjoint of
17 | the Global Eulerian–Lagrangian Coupled Atmospheric model (A-GELCA), which consists of an
18 | Eulerian National Institute for Environmental Studies global Transport Model (NIES-TM;
19 | Maksyutov et al., 2008; Belikov et al., 2011, 2013a, 2013b) and a Lagrangian particle
20 | dispersion model (FLEXPART; Stohl et al., 2005). This approach utilizes the accurate transport
21 | of the LPDM to calculate the signal near to the receptors, and ~~rapid~~efficient calculation of
22 | background responses using the adjoint of the Eulerian global transport model. In contrast to
23 | previous works (Rödenbeck et al., 2009; Rigby et al., 2011; Thompson and Stohl, 2014), in
24 | which the regional models were coupled at the spatial boundary of the domain, we
25 | implemented a coupling at ~~the a~~ time boundary in the global model domain (as described in
26 | Sect. 2.1). A-GELCA can be integrated into a variational inverse modeling system designed to
27 | optimize surface fluxes.

28 | The remainder of this paper is organized as follows. An overview of the coupled model is
29 | provided in Sect. 2, ~~and in.~~ In Sect. 3 we describe the variational inversion ~~process~~scheme. In
30 | Sect. 4 we address several problems regarding the coupled model that have not been covered
31 | previously (Ganshin et al., 2012). In Sect. 5 we describe the formulation and evaluation of the
32 | adjoint model. The computational efficiency of the adjoint model is analyzed in Sect. 6, and
33 | ~~finally~~ the conclusions are presented in Sect. 7.

1 4. Model and method

2 5.4.1. Global coupled Eulerian-Lagrangian model

3 In ~~the~~this paper we use a global Eulerian-Lagrangian coupled model, the principles of
4 which are described by Ganshin et al. (2012). ~~In this section we provide the formula~~The
5 coupled model consists of FLEXPART (version 8.0; run in backward mode) as the Lagrangian
6 particle dispersion model, and NIES TM (version NIES-08.1i) as the Eulerian off-line global
7 transport model. For concentration $C(x_r, t_r)$ (mole fraction) at receptor point x_r and time t_r ,
8 we provide the equation in its discrete form, as implemented in the model for the case of
9 surface fluxes:

$$10 \text{---} C(x_r, t_r) = \frac{Tm_{air}}{hNL\rho m_{CO_2}} \sum_{ij}^{IJ} \sum_{l=0}^L F_{ij}^l \sum_{n=1}^N f_{ij}^{ln} + \frac{1}{N} \sum_{ijk}^{IJK} C_{ijk}^B \sum_{n=1}^N f_{ijk}^n, \text{---} (1)$$

$$11 \text{---} C(x_r, t_r) = \frac{Tm_{air}}{hNS\rho m_{CO_2}} \sum_{ij}^{IJ} \sum_{s=0}^S F_{ij}^s \sum_{n=1}^N f_{ij}^{sn} + \frac{1}{N} \sum_{ijk}^{IJK} C_{ijk}^B \sum_{n=1}^N f_{ijk}^n, \text{---} (1)$$

12 where $i, j,$ and k are the indices that characterize the ~~position~~location of ~~the particle in~~
13 ~~the each grid~~ cell; l_s is the time index; ~~p is the particle index;~~ F_{ij}^l are the surface fluxes in
14 $kg \cdot m^{-2} \cdot s^{-1}$; C_{ijk}^B are the background concentrations ~~incalculated by~~ the Eulerian model at the
15 coupling time; f_{ijk}^n equals unity if the particle is within cell i, j, k , otherwise it equals zero; T
16 is the duration of the backward trajectory; L_S is the number of steps in time; N is the total
17 number of particles; h is the height up to which the effect of the surface fluxes is considered
18 significant; ρ is the average air density below height h ; and m_{air} and m_{CO_2} are the molar masses
19 of air and carbon dioxide, respectively. ~~The FLEXPART model starts at the observation point~~
20 ~~and calculates seven days' worth of backward trajectories for 1000 air particles, which are~~
21 ~~dispersed under the influence of turbulent diffusion. The background grid values of the~~
22 ~~concentrations, which are interpolated to the final points of the back trajectories, are~~
23 ~~transferred to the observation point and are the second term in the right hand side of Eq. (1).~~
24 The first term in this formula describes the contribution of the nearby sources of the
25 ~~component~~ considered component; these sources are located along the trajectories inside
26 layer h (500 m). The value of the first term is proportional to the flux in each cell along the
27 trajectory, and to the time during which the air particle is inside this cell (Ganshin et al.,
28 2013). ~~We implemented a coupling at the time boundary in the global domain~~2012). The
29 background grid values of the concentrations (calculated by the Eulerian model), which are
30 interpolated to the final points of the backward trajectories, are transferred to the

1 observation point and are the second term in the right-hand side of Eq. (1). The FLEXPART
2 model starts simulation at the observation point and calculates seven-day backward
3 trajectories for 1000 air particles, which are dispersed under the influence of turbulent
4 diffusion. The number of particles has been chosen to optimize the computational cost
5 without compromising the quality of modeling by Ganshin et al., (2013). The scheme of
6 concentration calculation for the given location includes coupling of two model approaches.
7 NIES TM calculates global concentrations for the selected time period (usually 1 year to
8 exclude spin-up effect), but stops 7 days before the time of the observations. To obtain the
9 concentrations for the observation time we transport the background concentrations from
10 NIES TM gridbox to the location of observation point along the trajectory ensemble calculated
11 by FLEXPART model and add contribution from surface sources. Therefore we have
12 implemented the coupling at a time boundary in the global domain of the NIES transport
13 model, while nested regional modeling systems such as one by Rodenbeck et al (2009) have to
14 couple at both region boundary and time boundary.

15 ~~The coupled model consists of FLEXPART (version 8.0; run in backward mode) as the~~
16 ~~Lagrangian particle dispersion model, and NIES TM (version NIES-08.1i) as the Eulerian off-~~
17 ~~line global transport model to calculate the background CO₂ values.~~

18 **5.1. NIES transport model**

19 Since the first publication of the GELCA model in 2012, the NIES transport model has
20 undergone significant updates. We provide a brief outline of the major features of the current
21 model. NIES TM is a global three-dimensional CTM that simulates the global distribution of
22 atmospheric tracers between the Earth's surface and a pressure level of 5 hPa. The
23 ~~model's~~model employs the standard horizontal latitude–longitude grid with reduced number
24 of meshes towards the poles and a spatial resolution of $2.5^\circ \times 2.5^\circ$ near the equator (Belikov et
25 al., 2011). The vertical coordinate is a flexible hybrid sigma–isentropic (σ – θ) with 32 levels
26 (Belikov et al., 2013b). To parameterize turbulent diffusivity we ~~follows~~follow the method
27 proposed by Hack et al. (1993), with a separate evaluation of transport processes in the free
28 troposphere and the planetary boundary layer (PBL). The PBL heights are provided by the
29 European Centre for Medium-Range Weather Forecasts (ECMWF) ERA-Interim reanalysis.
30 The modified Kuo-type parameterization scheme is used for cumulus convection (Belikov et
31 al., 2013a).

32 Inverse modeling assumes that the model reasonably well reproduces the relationship
33 between atmospheric mixing ~~ratio~~ratio and surface fluxes, assuming that the biases between

1 the simulated and observed concentrations are mostly due to the emission inventories errors.
2 To ensure that this is the case, the NIES TM model has been evaluated extensively, ~~and it~~
3 ~~consistently performs well in intercomparisons. Comparisons~~ against SF₆ and CO₂ (Belikov et
4 al., 2011, 2013b), CH₄ (Patra et al., 2011; Belikov et al., 2013b), and ²²²Rn (Belikov et al.,
5 2013a) measurements show the model ability to reproduce seasonal variations,
6 interhemispheric gradient and vertical profiles of tracers.

7 5.2.4.2. FLEXPART

8 FLEXPART ~~similar to, like~~ other LPDMs ~~consider, considers~~ atmospheric tracers as a
9 ~~discrete phase clouds of individual particles~~ and tracks ~~pathways~~ the pathway of each
10 ~~individual~~ particle. The advantage of this approach is the direct estimation of the sensitivity of
11 the measurements to the neighboring ~~sinks~~ sinks and sources by ~~running~~ tracking the particles
12 ~~back~~ backward in time. Usually it is ~~enough~~ sufficient to simulate for a limited number of days
13 (2-10) to determine, where particles intercept the surface layer before they spread vertically
14 and horizontally.

15 5.3.4.3. Meteorological data

16 To run both models we use reanalysis ~~which combines~~ dataset combining the Japanese
17 25-yr Reanalysis (JRA-25) and the Japanese Meteorological Agency Climate Data Assimilation
18 System (JCDAS) dataset (Onogi et al., 2007). The JRA-25/JCDAS dataset is distributed on a
19 Gaussian T106 grid ~~T106~~ with horizontal resolution 1.25° × 1.25°, 40 sigma-pressure levels
20 and in 6-~~hour~~ hour time steps. The use of JRA-25/JCDAS data for Eulerian and Lagrangian models
21 provides ~~a~~ consistency in the calculated fields; however, some features of FLEXPART and NIES
22 TM require different methods for processing the meteorological data.

23 5.3.1.4.3.1. Meteorological data processing for NIES TM

24 Isolation of the transport equations is an effective way to save a significant amount of
25 CPU time during tracer transport simulation. At the preprocessing stage, the NIES TM core
26 produced a static archive of advective, diffusive, and convective mass fluxes with time step
27 similar to the one of the original JRA-25/JCDAS data (6 hour). After that the archive is used by
28 an “offline” model specially designed only for passive transport of tracer. Intermediate fluxes
29 are derived by interpolation.

30 Besides the mass fluxes, the static archives contain fields of temperature, pressure,
31 humidity, vertical grid parameters (variation of the sigma-isentropic vertical coordinate over

1 time), and others. The pre-calculated and stored data field can be used directly for any of the
2 inert tracers. It is also possible to simulate chemically active tracers if the chemical reaction
3 can be written in the simplified linear decay form; e.g., for ^{222}Rn , CH_4 . Approximately 20 3-
4 dimensional and 1-dimensional arrays are written to a hard disk for every record. This
5 comprises around 10 GB of data per modelled month for the model's standard resolution of
6 $2.5^\circ \times 2.5^\circ$.

7 5.3.2.4.3.2. *Meteorological data processing for FLEXPART*

8 Originally, FLEXPART was driving driven by ECMWF reanalysis dataset distributed on a
9 grid with regular latitude–longitude horizontal structure and sigma–pressure vertical
10 coordinate. ~~Current~~The current version of the model was adapted to use JRA-25/JCDAS data,
11 by horizontal bilinear interpolation of the required parameters from a Gaussian grid to a
12 regular 1.25×1.25 grid. The vertical structure and temporal resolution of ~~of~~JRA-25/JCDAS
13 data were used without modification.

14 Given the large differences in structure, resolution and parameter estimation
15 ~~method~~methods used in different reanalysis dataset, the use of the same meteorology for both
16 Eulerian and Lagrangian models ~~is a~~provides significant benefit.
17

6.5. Inverse modeling for the flux optimization problem

Although the variational inversion method ~~theory~~ for minimizing the discrepancy between modeled and observed mixing ratios has been well described and published (i.e. Chevallier et al., 2005), we summarize it here.

The aim of the ~~inverseinversion~~ problem is to find the value of a state vector \mathbf{x} with n elements that minimizes ~~athe~~ cost function $J(\mathbf{x})$ ~~using a least-squares method:~~:

$$J(\mathbf{x}) = \frac{1}{2}(\mathbf{x} - \mathbf{x}_b)^T \mathbf{B}^{-1}(\mathbf{x} - \mathbf{x}_b) + \frac{1}{2}(\mathbf{H}\mathbf{x} - \mathbf{y})^T \mathbf{R}^{-1}(\mathbf{H}\mathbf{x} - \mathbf{y}),$$

$$J(\mathbf{x}) = \frac{1}{2}(\mathbf{x} - \mathbf{x}_b)^T \mathbf{B}^{-1}(\mathbf{x} - \mathbf{x}_b) + \frac{1}{2}(\mathbf{H}\mathbf{x} - \mathbf{y})^T \mathbf{R}^{-1}(\mathbf{H}\mathbf{x} - \mathbf{y}), \quad (2)$$

where \mathbf{y} is a vector of observations with m elements, and the matrix \mathbf{H} represents the forward model simulation mapping the state vector \mathbf{x} to the observation space. Here, ~~\mathbf{R}~~ \mathbf{R} is the covariance matrix (size $m \times m$) for observational error, which includes instrument and representation errors. The matrix ~~\mathbf{R}~~ \mathbf{R} also includes errors of the forward model \mathbf{H} . ~~\mathbf{B}~~ \mathbf{B} is the covariance matrix (size $n \times n$) of error for prior information of the state vector \mathbf{x}_b . ~~UseThe~~ use of the cost function in the form of Eq. (2) assumes that all errors ~~must~~ have Gaussian statistics and ~~beare~~ unbiased (Rodgers, 2000).

~~For linear \mathbf{H} ,~~ The minimization of the cost function (Eq. 2) has an analytic solution ~~involvingthat involves~~ a matrix inversion. If the Jacobian \mathbf{H} is available this analytic solution can implemented, unless the matrix sizes are too large for the available computing resources. Alternatively, Eq. 2 can be solved through an iterative minimization algorithm. In this case, the existence of the gradient of $J(\mathbf{x})$ with respect to \mathbf{x} allows using of powerful gradient algorithms for ~~minimisation~~ minimization. This gradient is efficiently provided by the adjoint (Giering and Kaminski, 1998; Kaminski et al., 1999; Chevallier et al., 2005; ~~Kopacz et al., 2009~~).

7.6. Assessment of the coupled model

The effect of different horizontal resolutions on Eulerian models is discussed in detail by Patra et al. (2008). In general, higher resolution helps to resolve a more detailed distribution of the tracer. However, the use of a ~~more detailed~~ higher resolution grid leads to additional computational cost, which is not always justified by the resulting model output. ~~This is~~ Higher resolution does not produce better results largely due to the limited availability of high-resolution meteorology and tracer emission datasets.

The paper by Ganshin et al. (2012) ~~in various test showed that~~ describing the

1 ~~coupled~~development of the GELCA model ~~surpasses the Eulerian~~provides a model in 4-month
2 ~~simulation~~testing report. The advantage of GELCA in reproducing the high-concentration
3 spikes and short-term variations caused mainly by anthropogenic emissions is more vivid
4 ~~with use of~~when using high resolution (1 km × 1 km) surface fluxes compared to standard
5 ~~low-resolution~~ (1° × 1°) fluxes. ~~However those tests considered only short 4-month~~
6 ~~simulations for a limited number of locations.~~

7 We ~~repeated~~expanded the comparison undertaken by Ganshin et al. (2012) ~~for~~to a two-
8 year period using an updated set of prescribed fluxes, which combines four components
9 similar to ~~the~~ analysis performed by Takagi et al., (2011) and Maksyutov et al., ~~(2012, (2013):~~
10 (a) anthropogenic fluxes from the Open source Data Inventory of Anthropogenic CO₂ (ODIAC;
11 Oda and Maksyutov, 2011) and the Carbon Dioxide Information Analysis Center's (CDIAC;
12 Andres et al., 2009, 2011) datasets; (b) biosphere fluxes simulated by the Vegetation
13 Integrative Simulator for Trace gases (VISIT) terrestrial biosphere model (Ito, 2010; Saito et
14 al., 2011, 2013); (c) oceanic fluxes predicted by ~~a~~ data assimilation system based on the
15 Offline ocean Tracer Transport Model (OTTM; Valsala and Maksyutov, 2010); and (d) biomass
16 burning emissions from the Global Fire Emissions Database (GFED) version 3.1 (van der Werf
17 et al., 2010). Biosphere fluxes have daily time step, while ~~the~~ others are monthly. ~~The initial~~
18 ~~global CO₂ distribution was obtained from GLOBALVIEW-CO₂ (2014).~~

19 We considered several cases with different model resolutions. For NIES TM we tested
20 grids at 10.0°, 2.5°, and 1.25° resolutions, with FLEXPART running at 1.0° (Table 1). The
21 resolution of the input fluxes was matched to that of FLEXPART. ~~Modeled~~Model results were
22 compared with ~~observations from the World Data Centre for Greenhouse Gases (WDCGG~~
23 ~~2015) and~~ the Siberian observations obtained by the Center for Global Environmental
24 Research (CGER) of the National Institute for Environmental Studies (NIES) and the Russian
25 Academy of Science (RAS), from ~~sevensix~~ tower sites (JR-STATION) as described ~~in Table 2~~
26 ~~by~~ Sasakawa et al., (2010). ~~The selected site locations are shown in Fig. 1.~~

27 ~~Although the total number of observational stations contributing to the WDCGG is about~~
28 ~~several hundreds, the set of sites conducting continuous (high temporal resolution is needed~~
29 ~~for the coupled model) observations is much smaller. We selected 19 sites (Table 2). Most of~~
30 ~~them are concentrated in the temperate latitudes of the northern hemisphere, where the~~
31 ~~variations in CO₂ concentration are most noticeable.~~

32 Siberia is assumed to be a substantial source and sink of CO₂-emissions, with high
33 uncertainties in the fluxes describing them (McGuire et al., 2009; Hayes et al., 2011; Saeki et

1 al., 2013). As a result, CTMs tend to reproduce the ~~interseasonal~~interannual variability of CO₂
2 quite poorly. We selected six tower JR-STATION sites to check the model performance in the
3 Siberian region (Table 3).

4 The analyzed sites are divided into three groups. The first group includes remote and
5 marine sites (ALT, AMS, BRW, CPT, IZO, JBN, MLO, MNM, ZEP) with very weak influence of
6 local sources, so the seasonal variation of CO₂ is controlled by global, large-scale variations.
7 For these sites contribution by using the Lagrangian component is negligible (see Fig. 2-4
8 panel b to analyze the difference between the coupled and the Eulerian models).

9 The second group includes sites with domination of long term variability of CO₂ and
10 relatively smooth and weak short term variations. Typically, these sites are located on the
11 border of two regions with very different fluxes (AMY, CMN, MHD, PAL, PRS, YON).

12 The sites selected to the third group are strongly influenced by local emissions and
13 global transport at the same time. Therefore the CO₂ concentration variation is controlled by
14 the strength and direction of wind, the depth of the boundary layer and other factors. Such
15 sites are mainly in the northern mid-latitudes (HUN, PUY, SSL, WSA) including all Siberian
16 towers (DEM, IGR, KRS, NOY, VGN, YAK). For these locations contributions of the Eulerian and
17 Lagrangian components are comparable. Therefore, the coupled model introduces the most
18 significant improvement when simulating CO₂ for these sites.

19 Figures 2 and 3 compare~~5 compares~~ the coupled and Eulerian model results with ~~tower~~
20 observations from the Igrim and Vaganovo.~~Recent towers. The recent~~ modifications
21 ~~(indicated in Sect. 2.2) mean that have significantly improve~~ the performance of NIES TM ~~is~~
22 ~~significantly improved~~ compared with the results reported by Ganshin et al. (2012). However,
23 ~~in this case compared to the updated NIES TM~~ the coupled model ~~reproduces the~~
24 ~~observations is~~ better ~~than the Eulerian model used on its own, providing areproducing short~~
25 ~~term peaks of concentration. This explains the observed reduction of the mean bias and STD~~
26 ~~(up to 1.5 ppm), and the~~ better simulation of the seasonal variation ~~(in phase and its~~
27 ~~amplitude. The standard deviation of the coupled).~~ The improvements in the CO₂ simulations
28 ~~due to the addition of the Lagrangian component to the Eulerian~~ model ~~misfit to the~~
29 ~~observations is around 0.5 ppm smaller. Moreover, the version of the coupled model with a~~
30 ~~very coarse grid of NIES TM (10.0°) outperforms the are higher- than those obtained by~~
31 ~~increasing the resolution versions~~ of the Eulerian NIES transport model (Table 3 Fig. 2-4).
32 Given the huge difference in computation costs between NIES TM for low- and high-resolution
33 grids (i.e. a difference by a factor of ~15 between grids with resolution 10.0° and 2.5°), the

1 advantage of the GELCA model is clear. Performance is important, as the setup considered
2 here is almost identical to ~~the case that~~ used in the inverse modeling of CO₂.

3 ~~However, improvements in CO₂ simulation due to the implementation of the GELCA~~
4 ~~model were obtained not for all the considered sites.~~ This ~~case~~ shows that ~~further~~
5 ~~modification of the setup (i.e. more detail meteorological data, switch to higher resolution) is~~
6 ~~necessary. Nevertheless,~~ the coupled model is ~~an~~ effective ~~even in the case of multiple limiting~~
7 ~~factors, such as high uncertainty of fluxes, a small number way to improve simulation of~~
8 ~~observations, and CO₂ without increasing~~ the ~~low~~ resolution of the Eulerian model. We
9 recognize that ~~the is quite problematic to use of the concentrations simulated from~~ the highly
10 uncertain surface fluxes to ~~judge simulate the tracer concentrations and use these~~
11 ~~concentrations for estimating~~ the quality of different model configurations ~~is quite~~
12 ~~problematic.~~ Nevertheless, we cannot improve our analysis, because we do not have
13 concentration measurements for tracers ~~with more accurate whose surface fluxes are more~~
14 ~~accurately known~~, like SF₆.

15 **8.7. Construction and validation of the adjoint model**

16 **8.1.7.1. Construction**

17 In this section, we present the development of the adjoint of the coupled model.
18 ~~Construction~~ ~~The incorporation~~ of the ~~adjoint to the~~ Lagrangian ~~part~~ ~~component~~ does not
19 require any modification to the code, as LPDMs are ~~able to track a significant number of~~
20 ~~particles backwards in time and thereby calculate the sensitivity of observations to the~~
21 ~~neighboring emissions areas.~~

22 ~~self-adjoint.~~ The development of the adjoint ~~to of~~ the Eulerian part is more complicated.
23 We decided to develop a discrete adjoint of NIES TM in order to make it consistent with the
24 forward model. An alternative approach is ~~at the~~ construction of ~~a~~ continuous adjoint derived
25 from the leading equations of the forward model (Giles and Pierce, 2000). The main
26 advantage of the discrete adjoint model is that the resulting gradients of the numerical cost
27 function are exact, even for nonlinear or iterative algorithms, ~~making them and this makes~~
28 ~~easier to validate, as validation of~~ the adjoint model, ~~which~~ is an essential and complicated
29 task.

30 The ~~tangent linear and~~ adjoint ~~models~~ ~~model~~ for NIES TM ~~were~~ ~~was~~ ~~created manually to~~
31 ~~achieve maximum computational efficiency, while the adjoint of NIES TM to FLEXPART~~
32 ~~coupler was~~ created using the Transformation of Algorithms in Fortran (TAF) software

1 (<http://www.FastOpt.com>). ~~Use~~ However, the use of this tool required some manual
2 treatment of the code. ~~We~~ TAF successfully produces the tangent linear and adjoint code of
3 individual procedures, but it gets confused when the model has complex structures (such as
4 loops and conditional operators). Therefore we often manually ~~redesign~~ redesigned and
5 ~~optimize~~ optimized the automatically generated adjoint code to optimize the efficiency ~~and~~,
6 improve readability and clarity of the adjoint model ~~and optimize the performance of~~
7 ~~computing using MPI, as the TAF code used here (version 1.5) do not fully support MPI~~
8 ~~routines~~.

9 The advantages of our coupled adjoint model are as follows.

- 10 1. Simple ~~construction~~ incorporation of the Lagrangian part ~~of the adjoint, as, since no~~
11 modification of ~~the~~ LPDM is ~~not~~ required. Potentially, NIES TM can be coupled to any
12 Lagrangian model.
- 13 2. ~~Minimizing~~ Minimization of the simulation time can be obtained, as once calculated ~~the~~
14 output from the Lagrangian model is applicable for different long-lived tracers.
- 15 3. Reduction of aggregation errors can be achieved, as the sensitivity for small regions and
16 even individual model cells near to observation sites is estimated using the LPDM part,
17 while the sensitivity for large regions ~~remoted~~ remote from the monitoring sites is
18 derived using the Eulerian part (Kaminski et al., 2001).
- 19 4. ~~Minimizing~~ Minimization of the computational cost can be obtained, as high-resolution
20 simulation are performed over ~~a~~ limited number of regions nearby to the observational
21 sites using the LPDM part, while for the rest of the globe the coarse-resolution results
22 are calculated by the Eulerian part.
- 23 5. High consistency of ~~calculated~~ the tracer ~~field~~ fields calculated by ~~the~~ Lagrangian and ~~the~~
24 Eulerian models due to ~~the fact that both models use~~ of the same ~~input~~ input
25 meteorology.

26 ~~The main drawback of the method is that the deriving of discrete adjoint of Eulerian~~
27 ~~model is a significant technical challenge.~~

28 **8.2.7.2. Validation of the coupled adjoint**

29 An essential stage of the adjoint model construction is ~~its~~ validation. A lack of accuracy
30 in the adjoint model ~~is~~ will likely ~~to~~ degrade the performance of the ~~minimisation of cost~~
31 ~~function minimization~~ (Eq. 2-). Several different tests were carried out to evaluate the

accuracy and precision of the constructed adjoint model ~~calculation~~. Considering the simple formulation of the ~~adjoint for the~~ Lagrangian part, we focused on testing the NIES TM adjoint.

~~8.2.1.7.2.1.~~ Validation of the NIES TM adjoint

The discrete adjoint obtained through automatic differentiation can be easily validated by comparing the adjoint sensitivities with forward model gradients calculated using the finite difference approximation (Henze et al., 2007).

~~Forward~~ The forward model sensitivity, λ_F , is calculated using the one- or two-sided finite difference equation,

$$\lambda = \frac{M'(x + \varepsilon) - M'(x)}{\varepsilon} \quad (3)$$

$$\lambda = \frac{M'(x + \varepsilon) - M'(x - \varepsilon)}{2\varepsilon} \quad \lambda_F = \frac{M'(x + \varepsilon \cdot x_e) - M'(x)}{\varepsilon \cdot x_e} \quad (3)$$

$$\lambda_F = \frac{M'(x + \varepsilon \cdot x_e) - M'(x - \varepsilon \cdot x_e)}{2\varepsilon \cdot x_e} \quad (4)$$

where M' denotes the tangent linear model, x_e is the part of x that contains the emissions (that is, the part that does not contain the initial mole fraction condition). During the calculations we perturbed several components of the x_e vector. A range of $\varepsilon = 0.1-0.01$ was proved in most cases to give an optimal balance between truncation and roundoff error (Henze et al., 2007).

In the first test, ~~forward~~ adjoint simulations were carried out with using an initial CO₂ distribution ~~and~~, zero surface flux for 2 days using (1-2 January 2010) and a horizontal grid with resolution $2.5^\circ \times 2.5^\circ$. ~~Adjoint simulations were then performed with CO₂ distribution perturbed by 1 ppm per grid cell~~. The adjoint gradient was then compared with that from the finite difference calculated using Eq. (3). This equation was selected in order to save CPU time by minimizing the number of forward model function ~~calculation for the~~ calculations. For this test we used $\varepsilon = 0.01$.

To quantify the difference between the two calculations of the sensitivity λ , we define the local relative error

$$E(lon, lat) = \frac{|\lambda_A - \lambda_F|}{\max \lambda_A}, \quad (5)$$

$$E(lon, lat) = \frac{|\lambda_A - \lambda_F|}{\max \lambda_A}, \quad (5)$$

1 where the subscripts A and F refer to adjoint and finite difference respectively, whereas lon,
 2 and lat refer to longitude and latitude ~~correspondently, respectively.~~ Figure 3e6c shows
 3 $E(lon, lat)$ with a logarithmic color scale. The sensitivities obtained byfor the adjoint have
 4 maximum relative error of order 10^{-16} , indicating that transport in the NIES TM adjoint is
 5 correct over short timescales. The overall comparisons did not seriously ~~changed~~change if we
 6 select ~~a~~ different grid cells or use ~~various~~other values of ϵ .

7 The definition of the adjoint of the tangent linear forward model M^* requires that for an
 8 inner product ~~$\langle \cdot, \cdot \rangle$~~ $\langle \cdot, \cdot \rangle$ and two random vectors \mathbf{u} and \mathbf{v} , the following expression should ~~be~~
 9 validhold:

$$10 \quad \forall \mathbf{u}, \forall \mathbf{v} \quad \langle M' \mathbf{u}, \mathbf{v} \rangle = \langle \mathbf{u}, M^* \mathbf{v} \rangle. \quad \forall \mathbf{u}, \forall \mathbf{v} \quad \langle M' \mathbf{u}, \mathbf{v} \rangle = \langle \mathbf{u}, M^* \mathbf{v} \rangle. \quad (6)$$

11 For practical use the identity in Eq. (6) is ~~reworded~~rewritten as follows (Wilson et al.,
 12 2014):

$$13 \quad \frac{\|M'(\mathbf{u})\|^2}{(\mathbf{u}, M^*(M(\mathbf{u})))} = 1. \quad (7)$$

$$14 \quad \frac{\|M'(\mathbf{u})\|^2}{(\mathbf{u}, M^*(M'(\mathbf{u})))} = 1. \quad (7)$$

15 We use Eq. (7) to test the adjoint model initialized using several different random
 16 ~~setups~~random vectors \mathbf{u} and \mathbf{v} . For all cases, Eq. (7) compares well ~~with~~within machine
 17 epsilon with mismatch between $-3e^{-14}$ to $6e^{-14}$.

19 ~~8.2.2.7.2.2.~~ Real case simulation

20 The next series of calculations was made for real measurements. ~~As in the first part of~~
 21 ~~the article, we~~We used data from the Siberian observation network ~~(Table 2)(Table 3)~~
 22 period 1–4 January 2010. ~~The NIES adjoint was simulated with a horizontal resolution of 2.5°~~
 23 ~~$\times 2.5^\circ$, CO_2 initial conditions~~ and ~~the Lagrangian response was simulated with a horizontal~~
 24 ~~fluxes were the same as those used for the CELGA forward simulations in Section 4. We run A-~~
 25 ~~GELCA using grids of 10.0° and 2.5° for Eulerian part and of 1.0° for Lagrangian component~~
 26 ~~(similar to Cs-1 and Cs-2 in Table 1) and considered several cases.~~

27 The sensitivities of CO_2 concentrations were calculated using the Eulerian component
 28 only in Figs. 7,8 a) (resolution of 2.5°), b) (resolution of $1.0^\circ \times 1.0^\circ$).

1 ~~Figure 4 shows the sensitivity calculated with the Eulerian component, while Fig. 5~~
2 ~~shows the same but 10.0°), using the Lagrangian component. Although the contours of the~~
3 ~~two figures coincide, it is clear only in Figs. 7,8 c)(resolution of 1.0°), and d) (resolution of~~
4 ~~1.0°, but aggregated on a grid with resolution of 2.5°), and using the coupled adjoint model in~~
5 ~~Fig. 7,8 e) (Eulerian component at a resolution of 2.5° and the Lagrangian component~~
6 ~~aggregated on the grid with a resolution of 2.5°), and f) (as for e) , but the resolution of the~~
7 ~~Eulerian adjoint model was 10.0°). Figure 7 corresponds to the 2-nd day of simulation, while~~
8 ~~Figure 8 is for 4-th day.~~

9 ~~Above, we have already stated that the Eulerian part of the coupled model is more~~
10 ~~effective in reproducing of long-term patterns, while the Lagrangian part is better for~~
11 ~~resolving synoptic and hourly variations. This follows from the fact that the A-GELCA~~
12 ~~components have different footprints. The Eulerian adjoint has a wider footprint, with the~~
13 ~~greatest valuevalues in an area where the effect of all stations is summed. In this case, most of~~
14 ~~the stations can be outside this zone, as the The Euler model monitors global and large-scale~~
15 ~~changes. This figure illustrates, although some stations can be outside this zone (i.e. YAK, at~~
16 ~~Fig. 7a,g or NOY, at Fig. 8a,b). These figures illustrate why the Eulerian model, even with a~~
17 ~~sufficiently detailed grid, is unablefails to reproduce CO₂ variations (Sect. 4). The footprint~~
18 ~~width decreases when the NIES TM resolution is increased, but the value of the sensitivity~~
19 ~~increases with resolution.~~

20 The FLEXPART model sensitivity shows more irregular distributions, and higher values
21 closer to the observational sites, thereby reflecting the model's ability to monitor small-scale
22 changes. (Fig. 7-8 panels c,d).

23 During coupling, the sensitivity is aligned due to the crosslinking of components (Fig.
24 ~~67-8 panels e,f~~). Thus, ~~the~~ intensity has a maximum near the stations and smoothly decreases
25 ~~with increasingwhen~~ distance ~~increases~~. The Eulerian and Lagrangian models employ
26 different approaches and grid resolutions for the modeling of atmospheric tracers, and can
27 thus resolve processes with different time and spatial scales, and underlying physics.

28 ~~Figure 7 shows the sensitivity calculated for the same setup as for Fig. 6, but using NIES~~
29 ~~TM with a 10.0° resolution.~~ By changing the Eulerian model resolution, it is possible to change
30 size of the footprint. This system can utilize responses calculated at higher resolutions, such
31 as 0.5° or 0.1°, but these setups require more accurate driving data and regular observations
32 available for smaller time steps.

33

9.8. Computational efficiency

We tested several different methods to reduce the computational ~~burden~~cost of the adjoint model. First, the Eulerian part of the adjoint model was driven by static archives of meteorological parameters, as described in Sect. 2.4.1. Second, the forward NIES model was altered so that at each model timestep it saved any variables that ~~would~~were also ~~be~~-needed by the adjoint model. ~~These~~Therefore, these variables ~~therefore~~-did not have to be recalculated for ~~use~~being used in the adjoint model. (This was possible because we used a discrete version of the adjoint, which was fully compatible with the forward model). Third, the Lagrangian part of the adjoint model made use of pre-calculated response functions, as described in Sect. 2.4.2.

To run the adjoint model we used a Linux workstation with 8 Intel(R) Xeon(R) E5-4650 ~~2.70GHz~~70 GHz processors and 64 GB of RAM. The CPU time of the adjoint model (backward only) ~~is~~was almost equal to CPU time required to run the forward model. It ~~take~~took about 1.3 min for a ~~week~~long iteration (forward and backward). The memory demand ~~is~~was about 1 GB. Henze et al. (2007) reports that the ratio between simulation time in backward and forward modes for adjoint models derived for other CTMs, as follows: GEOS-Chem: 1.5, STEM: 1.5, CHIMERE: 3–4, IM-AGES: 4, Polair: 4.5–7, and CIT: 11.75. Thus, the adjoint of the developed coupled model GELCA is quite efficient. To achieve this level of efficiency, a substantial amount of manual programming effort is required, despite the automatic code generated by TAF. The main disadvantage of TAF is that many redundant recomputations are often generated by the compiler. A crucial optimization of the adjoint code is required to eliminate these extra recomputations.

10.9. Summary

In this ~~papers~~paper we have presented the construction and evaluation of an adjoint of the global Eulerian–Lagrangian coupled model GELCA that will be integrated into a variational inverse system designed to ~~optimizing~~optimize surface fluxes. The coupled model combines the NIES three-dimensional transport model as its Eulerian part and the FLEXPART plume diffusion model as its Lagrangian component. The Eulerian and Lagrangian components are coupled at a time boundary in the global domain. The model was originally developed to study the carbon dioxide and methane atmospheric ~~distribution~~distributions.

The Lagrangian component did not require any code modification, as FLEXPART is ~~tracking~~a self-adjoint and ~~tracks~~ a significant number of particles ~~back~~backward in time, ~~and thereby calculates in order to calculate~~ the sensitivity of observations to the neighboring emissions areas. ~~Thus, construction of the adjoint to the Lagrangian part does not require any modification to the code.~~

For Eulerian part, the discrete adjoint was constructed directly from the original NIES TM code, ~~in contrast to a construction of~~instead of constructing a continuous adjoint derived from the forward model basic equations. The tangent linear and adjoint models of the ~~Eulerian model~~NIES TM to FLEXPART coupler were derived using the automatic differentiation software TAF (<http://www.FastOpt.com>), which significantly accelerated the development. However, considerable manual processing of forward and adjoint model codes was necessary to improve the transparency and clarity of the model and to optimize the computational performance of ~~computing~~, including MPI. ~~The, as the~~ TAF code used here (version 1.5) ~~did~~does not fully support MPI routines.

~~The Eulerian and Lagrangian adjoints were coupled at the time boundary in the global domain.~~The main benefit of the developed discrete adjoint is accurate calculation of the numerical cost function gradients, even if the algorithms are nonlinear. The overall advantages of the developed model also include relatively simple ~~construction~~incorporation of the ~~adjoint to the~~Lagrangian part and fast computation using the Lagrangian component, scalability of sensitivity calculation depending on distance to monitoring sites, thereby reducing aggregation errors, and computational efficiency even for high-resolution simulations.

The ~~accuracy of the~~transport scheme accuracy of the forward coupled model was investigated using ~~simulation of the~~ distribution of the atmospheric CO₂. The GELCA components and the model itself had previously been validated ~~in~~using various tests and by

1 comparison with ~~both~~ measurements and with other transport models for CO₂ and other
2 tracers. ~~Performed~~The analyses in the present paper ~~analyses showed,~~have shown that
3 GELCACELGA is effective in capturing the seasonal variability of atmospheric tracer at
4 observation sites. Decreasing of the Eulerian model resolution ~~are~~does not ~~able to~~
5 significantly distort the transport model performance; however, running the coupled model
6 using NIES TM with low resolution grid can maximize simulation speed and use of data
7 storage.

8 The Eulerian ~~and Lagrangian components of the~~ adjoint ~~model were~~was validated using
9 various tests in which the adjoint gradients were compared to gradients calculated with
10 numerical finite difference. We evaluated each ~~individual~~ routine of the discrete adjoint of the
11 Eulerian model and the adjoint gradients of the cost function. The ~~obtained~~ precision obtained
12 of the results ~~in~~of the considered numerical experiments demonstrates proper construction of
13 the adjoint.

14 The CPU time ~~of~~needed by the adjoint model is comparable with ~~that~~those of other
15 models, as we used several methods to reduce the computational ~~load~~cost. The forward NIES
16 model was altered so that at each model ~~timestep~~time step it saved ~~any~~all variables that
17 ~~would~~were also ~~be~~being needed by the adjoint model. These variables therefore did not have
18 to be recalculated for use in the adjoint model. In addition, the adjoint simulation was isolated
19 from the recalculation of NIES TM meteorological parameters and Lagrangian response
20 functions. All supplementary parameters ~~are~~were pre-calculated before running the adjoint
21 and ~~are~~were stored in static archives.

22 The developed ~~adjoint~~A-GELCA model will be incorporated into ~~variationa~~ variational
23 inversion system aiming studying greenhouse gases (mainly CH₄ and CO₂), by assimilating
24 tracer measurements from *in situ*, aircraft and remote sensing observations. However, before
25 performing real inverse modeling simulations it is necessary to select a proper minimization
26 program and find the optimal values for the error covariance matrices **R** and **B** ~~with the~~
27 optimal values.

28

1 **Code availability**

2 All code in the current version of the NIES forward model is available on request. Any
3 potential user interested in these modules should contact D. Belikov;
4 [\(\[dmitry.belikov@nies.go.jp\]\(mailto:dmitry.belikov@nies.go.jp\)\)](mailto:dmitry.belikov@nies.go.jp) or S. Maksyutov (shamil@nies.go.jp), and any feedback on the
5 modules is welcome. Note that ~~one~~that potential users may need help using the forward and
6 adjoint model effectively, but open support for the model is not available due to lack of
7 resources. The code of the adjoint part of the current NIES model is unavailable for
8 distribution, as it was generated using the commercial tool TAF (<http://www.FastOpt.com>).
9 However, we can provide the sources which were used as input for TAF.

10 The FLEXPART code was taken from the official web site <http://flexpart.eu/>. The
11 procedures necessary to run FLEXPART with the JCDAS reanalysis are also available upon
12 request.

13 **Acknowledgments**

14 The authors thank A. Stohl for providing the FLEXPART model. We also thank T.
15 Machida for Siberian observation data (downloaded from <http://db.cger.nies.go.jp/>). The JRA-
16 25/JCDAS meteorological datasets used in the simulations were provided by the Japan
17 Meteorological Agency. The WDCGG observation data used in the comparisons were provided
18 by The World Data Centre for Greenhouse Gases. We appreciate cooperation of the WDCGG
19 data providers listed in Table 2. The computational resources were provided by NIES. This
20 study was ~~performed~~supported by order of the Ministry for Education and Science of the
21 Russian Federation No. 5.628.2014/K-~~and was supported~~, by ~~The~~the Tomsk State University
22 Academic D.I. Mendeleev Fund Program in 2014–2015 and by GRENE Arctic project.

23

1 **References**

- 2 Andres, R. J., Boden, T. A., and Marland, G.: Annual fossil-fuel CO₂ emissions: Mass of emissions
3 gridded by one degree latitude by one degree longitude. Carbon Dioxide Information
4 Analysis Center, Oak Ridge National Laboratory, U.S. Department of Energy, Oak Ridge,
5 Tenn., U.S.A., doi 10.3334/CDIAC/ffe.ndp058.2009, 2009.
- 6 Andres, R. J., Gregg, J. S., Losey, L., Marland, G., Boden, T.: Monthly, global emissions of carbon
7 dioxide from fossil fuel consumption, *Tellus* 63B, 309–327, 2011.
- 8 Baker, D. F., Law, R. M., Gurney, K. R., Rayner, P., Peylin, P., Denning, A. S., Bousquet, P.,
9 Bruhwiler, L., Chen, Y.-H., Ciais, P., Fung, I. Y., Heimann, M., John, J., Maki, T., Maksyutov,
10 S., Masarie, K., Prather, M., Pak, B., Taguchi, S., and Zhu, Z.: TransCom 3 inversion
11 intercomparison: impact of transport model errors on the interannual variability of
12 regional CO₂ fluxes, 1988–2003, *Global Biogeochem. Cy.*, 20, GB1002,
13 doi:10.1029/2004GB002439, 2006.
- 14 [Basu, S., Guerlet, S., Butz, A., Houweling, S., Hasekamp, O., Aben, I., Krummel, P., Steele, P.,](#)
15 [Langenfelds, R., Torn, M., Biraud, S., Stephens, B., Andrews, A., and Worthy, D.: Global](#)
16 [CO₂ fluxes estimated from GOSAT retrievals of total column CO₂, *Atmos. Chem. Phys.*,](#)
17 [13, 8695-8717, doi:10.5194/acp-13-8695-2013, 2013.](#)
- 18 Belikov, D., Maksyutov, S., Miyasaka, T., Saeki, T., Zhuravlev, R., and Kiryushov, B.: Mass-
19 conserving tracer transport modelling on a reduced latitude-longitude grid with NIES-
20 TM, *Geosci. Model Dev.*, 4, 207–222, 2011.
- 21 Belikov, D. A., Maksyutov, S., Krol, M., Fraser, A., Rigby, M., Bian, H., Agusti-Panareda, A.,
22 Bergmann, D., Bousquet, P., Cameron-Smith, P., Chipperfield, M. P., Fortems-Cheiney, A.,
23 Gloor, E., Haynes, K., Hess, P., Houweling, S., Kawa, S. R., Law, R. M., Loh, Z., Meng, L.,
24 Palmer, P. I., Patra, P. K., Prinn, R. G., Saito, R., and Wilson, C.: Off-line algorithm for
25 calculation of vertical tracer transport in the troposphere due to deep convection,
26 *Atmos. Chem. Phys.*, 13, 1093–1114, doi:10.5194/acp-13-1093-2013, 2013a.
- 27 Belikov, D., Maksyutov, S., Sherlock, V., Aoki, S., Deutscher, N. M., Dohe, S., Griffith, D., Kyro, E.,
28 Morino, I., Nakazawa, T., Notholt, J., Rettinger, M., Schneider, M., Sussmann, R., Toon, G.
29 C., Wennberg, P. O., and Wunch, D.: Simulations of column-average CO₂ and CH₄ using the
30 NIES TM with a hybrid sigma–isentropic (σ – θ) vertical coordinate, *Atmos. Chem. Phys.*,
31 13, 1713–1732, doi:10.5194/acp-13-1713-2013, 2013b.
- 32 Bovensmann, H., Burrows, J. P., Buchwitz, M., Frerick, J., Noël, S., Rozanov, V. V., Chance, K. V.,
33 and Goede, A. P. H.: SCIAMACHY: Mission objectives and measurement modes, *J. Atmos.*
34 *Sci.*, 56, 127–150, 1999.
- 35 Bovensmann, H., Buchwitz, M., Burrows, J. P., Reuter, M., Krings, T., Gerilowski, K., Schneising,
36 O., Heymann, J., Tretner, A., and Erzinger, J.: A remote sensing technique for global
37 monitoring of power plant CO₂ emissions from space and related applications, *Atmos.*
38 *Meas. Tech.*, 3, 781–811, doi:10.5194/amt-3-781-2010, 2010.
- 39 Bruhwiler, L. M. P., Michalak, A. M., Peters, W., Baker, D. F., and Tans, P. P.: An improved

- 1 Kalman Smoother for atmospheric inversions, *Atmos. Chem. Phys.*, 5, 2691–2702,
2 doi:10.5194/acp-5-2691-2005, 2005.
- 3 Buchwitz, M., Reuter, M., Bovensmann, H., Pillai, D., Heymann, J., Schneising, O., Rozanov, V.,
4 Krings, T., Burrows, J. P., Boesch, H., Gerbig, C., Meijer, Y., and Löscher, A.: Carbon
5 Monitoring Satellite (CarbonSat): assessment of atmospheric CO₂ and CH₄ retrieval
6 errors by error parameterization, *Atmos. Meas. Tech.*, 6, 3477–3500, doi:10.5194/amt-
7 6-3477-2013, 2013.
- 8 Chevallier, F., Fisher, M., Peylin, P., Serrar, S., Bousquet, P., Bréon, F.-M., Chédin, A., and Ciais,
9 P.: Inferring CO₂ sources and sinks from satellite observations: method and application
10 to TOVS data, *J. Geophys. Res.*, 110, D24309, doi:10.1029/2005JD006390, 2005.
- 11 Crisp, D., Atlas, R. M., Bréon, F.-M., Brown, L. R., Burrows, J. P., Ciais, P., Connor, B. J., Doney, S.
12 C., Fung, I. Y., Jacob, D. J., Miller, C. E., O'Brien, D., Pawson, S., Randerson, J. T., Rayner, P.,
13 Salawitch, R. S., Sander, S. P., Sen, B., Stephens, G. L., Tans, P. P., Toon, G. C., Wennberg, P.
14 O., Wofsy, S. C., Yung, Y. L., Kuang, Z., Chudasama, B., Sprague, G., Weiss, P., Pollock, R.,
15 Kenyon, D., and Schroll, S.: The Orbiting Carbon Observatory (OCO) mission, *Adv. Space
16 Res.*, 34, 700–709, 2004.
- 17 [Deng, F., Jones, D. B. A., Henze, D. K., Bousseres, N., Bowman, K. W., Fisher, J. B., Nassar, R.,](#)
18 [O'Dell, C., Wunch, D., Wennberg, P. O., Kort, E. A., Wofsy, S. C., Blumenstock, T., Deutscher,](#)
19 [N. M., Griffith, D. W. T., Hase, F., Heikkinen, P., Sherlock, V., Strong, K., Sussmann, R., and](#)
20 [Warneke, T.: Inferring regional sources and sinks of atmospheric CO₂ from GOSAT XCO₂](#)
21 [data, *Atmos. Chem. Phys.*, 14, 3703-3727, doi:10.5194/acp-14-3703-2014, 2014.](#)
- 22 Elbern, H., Schmidt, H., and Ebel, A.: Variational data assimilation for tropospheric chemistry
23 modeling, *J. Geophys. Res.*, 102, 15,967–15,985, 1997.
- 24 Enting, I. G., and Mansbridge, J. V., Seasonal sources and sinks of atmospheric CO₂: Direct
25 inversion of filtered data, *Tellus B*, 41B, 111–126, doi: 10.1111/j.1600-
26 0889.1989.tb00129.x, 1989.
- 27 Enting, I. T.: *Inverse problems in atmospheric constituent transport*, Cambridge University
28 Press, Cambridge, UK, 2002.
- 29 Ganshin, A., Oda, T., Saito, M., Maksyutov, S., Valsala, V., Andres, R. J., Fisher, R. E., Lowry, D.,
30 Lukyanov, A., Matsueda, H., Nisbet, E. G., Rigby, M., Sawa, Y., Toumi, R., Tsuboi, K.,
31 Varlagin, A., and Zhuravlev, R.: A global coupled Eulerian-Lagrangian model and 1 × 1 km
32 CO₂ surface flux dataset for high-resolution atmospheric CO₂ transport simulations,
33 *Geosci. Model Dev.*, 5, 231–243, doi:10.5194/gmd-5-231-2012, 2012.
- 34 Giles, M. B., and Pierce, N. A.: An Introduction to the Adjoint Approach to Design, *Flow Turbul.*
35 *Combust.*, 65, 393–415, 2000.
- 36 Giering, R., and T. Kaminski, Recipes for adjoint code construction, *Trans. Math. Software*,
37 24(4), 437–474, doi:10.1145/293686.293695, 1998.
- 38 [GLOBALVIEW-CO₂ Cooperative Atmospheric Data Integration Project - Carbon Dioxide. CD-](#)
39 [ROM, NOAA ESRL, Boulder, Colorado \[Also available on Internet via anonymous FTP to](#)

- 1 | <ftp.cmdl.noaa.gov/Path:ccg/co2/GLOBALVIEW/>, 2014.
- 2 Gurney, K. R., Law, R. M., Denning, A. S., Rayner, P. J., Baker, D., Bousquet, P., Bruhwiler, L.,
3 Chen, Y.-H., Ciais, P., Fan, S., Fung, I., Gloor, M., Heimann, M., Higuchi, K., John, J., Maki, T.,
4 Maksyutov, S., Masarie, K., Peylin, P., Prather, M., Pak, B. C., Randerson, J. R., Sarmiento, J.,
5 Taguchi, S., Takahashi, T. and Yuen, C.-W.: Towards robust regional estimates of CO₂
6 sources and sinks using atmospheric transport models, *Nature*, 415, 626–630, 2002.
- 7 Gurney, K. R., Law, R. M., Denning, A. S., Rayner, P. J., Pak, B. C., Baker, D., Bousquet, P.,
8 Bruhwiler, L., Chen, Y.-H., Ciais, P., Fung, I. Y., Heimann, M., John, J., Maki, T., Maksyutov,
9 S., Peylin, P., Prather, M., and Taguchi, S.: Transcom 3 inversion intercomparison: model
10 mean results for the estimation of seasonal carbon sources and sinks, *Global*
11 *Biogeochem. Cy.*, 18, GB1010, doi:10.1029/2003GB002111, 2004.
- 12 Hack, J. J., Boville, B. A., Briegleb, B. P., Kiehl, J. T., Rasch, P. J., and Williamson, D. L.: Description
13 of the NCAR community climate model (CCM2), NCAR/TN-382, 108, 1993.
- 14 Haines, P. E., Esler, J. G., and Carver, G. D.: Technical note: Adjoint formulation of the TOMCAT
15 atmospheric scheme in the Eulerian backtracking framework (RETRO-TOM), *Atmos.*
16 *Chem. Phys.*, 14, 5477–5493, 2014.
- 17 Hayes, D. J., McGuire, A. D., Kicklighter, D. W., Gurney, K. R., Burnside, T. J., and Melillo, J. M.: Is
18 the northern high-latitude land-based CO₂ sink weakening?, *Global Biogeochem. Cycles*,
19 25, GB3018, doi:10.1029/2010GB003813, 2011.
- 20 Henze, D. K., Hakami, A., and Seinfeld, J. H.: Development of the adjoint of GEOS-Chem, *Atmos.*
21 *Chem. Phys.*, 7, 2413–2433, doi:10.5194/acp-7-2413-2007, 2007.
- 22 Hourdin, F., and Talagrand, O.: Eulerian backtracking of atmospheric tracers. I: Adjoint
23 derivation and parametrization of subgrid-scale transport, *Q. J. Roy. Meteor. Soc.*, 132,
24 585–603, 2006.
- 25 IPCC 2007: Climate change 2007: the physical science basis, in: Contribution of Working
26 Group I to the Fourth Assessment Report of the Intergovernmental Panel on Climate
27 Change (eds. Solomon, S., Qin, D., Manning, M., Chen, Z., Marquis, M., et al.), Cambridge
28 University Press, Cambridge, pp. 135–145.
- 29 Ito, A.: Changing ecophysiological processes and carbon budget in East Asian ecosystems
30 under near-future changes in climate: Implications for long-term monitoring from a
31 process-based model, *J. Plant Res.*, 123, 577–588, 2010.
- 32 Kaminski, T., Heimann, M., and Giering, R.: A coarse grid three-dimensional global inverse
33 model of the atmospheric transport: 1. Adjoint model and Jacobian matrix, *J. Geophys.*
34 *Res.*, 104(D15), 18,535–18,553, doi:10.1029/1999JD900147, 1999a.
- 35 Kaminski, T., Heimann, M., and Giering, R.: A coarse grid three-dimensional global inverse
36 model of the atmospheric transport: 2. Inversion of the transport of CO₂ in the 1980s, *J.*
37 *Geophys. Res.*, 104(D15), 18,555–18,581, doi:10.1029/1999JD900146, 1999b.
- 38 Kaminski, T., Rayner, P., Heimann, M., and Enting, I.: On aggregation errors in atmospheric
39 transport inversions, *J. Geophys. Res.*, 106(D5):4703, 2001.

- 1 [Karion, A., Sweeney, C., Wolter, S., Newberger, T., Chen, H., Andrews, A., Kofler, J., Neff, D., and](#)
2 [Tans, P.: Long-term greenhouse gas measurements from aircraft, *Atmos. Meas. Tech.*, **6**,](#)
3 [511-526, doi:10.5194/amt-6-511-2013, 2013.](#)
- 4 [Koyama, Y., Maksyutov, S., Mukai, H., Thoning, K., and Tans, P.: Simulation of variability in](#)
5 [atmospheric carbon dioxide using a global coupled Eulerian-Lagrangian transport](#)
6 [model, *Geosci. Model Dev.*, **4**, 317-324, doi:10.5194/gmd-4-317-2011, 2011.](#)
- 7 Kuze, A., Suto H., Nakajima M., and Hamazaki T.: Thermal and near infrared sensor for carbon
8 observation Fourier-transform spectrometer on the Greenhouse Gases Observing
9 Satellite for greenhouse gases monitoring, *Appl. Opt.*, **48**, 6716-6733,
10 doi:10.1364/AO.48.006716, 2009.
- 11 ~~[Kopacz, M., Jacob, D. J., Henze, D. K., Heald, C. L., Streets, D. G., and Zhang, Q.: Comparison of](#)~~
12 ~~[adjoint and analytical Bayesian inversion methods for constraining Asian sources of](#)~~
13 ~~[carbon monoxide using satellite \(MOPITT\) measurements of CO columns, *J. Geophys.*](#)~~
14 ~~[Res., **114**, D04305, doi:10.1029/2007JD009264, 2009.](#)~~
- 15 ~~[Koyama, Y., Maksyutov, S., Mukai, H., Thoning, K., and Tans, P.: Simulation of variability in](#)~~
16 ~~[atmospheric carbon dioxide using a global coupled Eulerian-Lagrangian transport](#)~~
17 ~~[model, *Geosci. Model Dev.*, **4**, 317-324, doi:10.5194/gmd-4-317-2011, 2011.](#)~~
- 18 Law, R. M., Rayner, P. J., Denning, A. S., Erickson, D., Fung, I. Y., Heimann, M., Piper, S. C.,
19 Ramonet, M., Taguchi, S., Taylor, J. A., Trudinger, C. M., and Watterson, I. G.: Variations in
20 modelled atmospheric transport of carbon dioxide and the consequences for CO₂
21 inversions, *Global Biogeochem. Cy.*, **10**, 783-796, 1996.
- 22 Law, R. M., Peters, W., Rödenbeck, C., Aulagnier, C., Baker, I., Bergmann, D. J., Bousquet, P.,
23 Brandt, J., Bruhwiler, L., Cameron-Smith, P. J., Christensen, J. H., Delage, F., Denning, A. S.,
24 Fan, S., Geels, C., Houweling, S., Imasu, R., Karstens, U., Kawa, S. R., Kleist, J., Krol, M. C.,
25 Lin, S.-J., Lokupitiya, R., Maki, T., Maksyutov, S., Niwa, Y., Onishi, R., Parazoo, N., Patra, P.
26 K., Pieterse, G., Rivier, L., Satoh, M., Serrar, S., Taguchi, S., Takigawa, M., Vautard, R.,
27 Vermeulen, A. T., and Zhu, Z.: TransCom model simulations of hourly atmospheric CO₂:
28 Experimental overview and diurnal cycle results for 2002, *Global Biogeochem. Cy.*, **22**,
29 GB3009, doi:10.1029/2007GB003050, 2008.
- 30 [Liu, J., Bowman, K. W., and Henze D. K.: Source-receptor relationships of column-average CO₂](#)
31 [and implications for the impact of observations on flux inversions. *J. Geophys. Res.*](#)
32 [Atmos., **120**, 5214-5236. doi: 10.1002/2014JD022914, 2015.](#)
- 33 Maki, T., Ikegami, M., Fujita, T., Hirahara, T., Yamada, K., Mori, K., Takeuchi, A., Tsutsumi, Y.,
34 Suda, K., and Conway, T. J., New technique to analyse global distributions of CO₂
35 concentrations and fluxes from non-processed observational data, *Tellus B*, **62**, 797-
36 809, doi:10.1111/j.1600-0889.2010.00488.x, 2010.
- 37 Maksyutov, S., Patra, P. K., Onishi, R., Saeki, T., and Nakazawa, T.: NIES/FRCGC Global
38 Atmospheric Tracer Transport Model: Description, validation, and surface sources and
39 sinks inversion, *J. Earth Simulator*, **9**, 3-18, 2008.

- 1 Maksyutov, S., Takagi, H., Valsala, V. K., Saito, M., Oda, T., Saeki, T., Belikov, D. A., Saito, R., Ito,
2 A., Yoshida, Y., Morino, I., Uchino, O., Andres, R. J., and Yokota, T.: Regional CO₂ flux
3 estimates for 2009–2010 based on GOSAT and groundbased CO₂ observations, *Atmos.*
4 *Chem. Phys.*, 13, 9351–9373. <http://dx.doi.org/10.5194/acp-13-9351-2013>, 2013.
- 5 Marchuk, G.: Numerical solution of the problems of the dynamics of the atmosphere and the
6 ocean (In Russian), *Gidrometeoizdat, Leningrad*, 303 pp., 1974.
- 7 Marchuk, G. I.: Adjoint equations and analysis of complex systems, Series: Mathematics and its
8 applications, v. 295, Kluwer Academic Publishers, Dordrecht and Boston, 484 pp., 1995.
- 9 McGuire, A. D., Anderson, L. G., Christensen, T. R., Dallimore, S., Guo, L. D., Hayes, D. J.,
10 Heimann, M., Lorenson, T. D., Macdonald, R. W., and Roulet, N.: Sensitivity of the carbon
11 cycle in the Arctic to climate change, *Ecol. Monogr.*, 79(4), 523–555, doi:10.1890/08-
12 2025.1, 2009.
- 13 ~~Meirink, J. F., Bergamaschi, P., Frankenberg, C., d'Amelio, M. T. S., Dlugokencky, E. J., Gatti, L. V.,~~
14 ~~Houweling, S., Miller, J. B., Roeckmann, T., Villani, M. G., and Krol, M. C.: Four-dimensional~~
15 ~~variational data assimilation for inverse modeling of atmospheric methane emissions:~~
16 ~~Analysis of SCIAMACHY observations, *J. Geophys. Res.*, 113, doi:10.1029/2007JD009740,~~
17 ~~2008.~~
- 18 ~~Müller, J. F., and Stavrakou, T.: Inversion of CO and NO_x emissions using the adjoint of the~~
19 ~~IMAGES model, *Atmos. Chem. Phys.*, 5, 1157–1186, doi:10.5194/acp-5-1157-2005, 2005.~~
- 20 Oda, T., and Maksyutov, S.: A very high-resolution (1 km × 1 km) global fossil fuel CO₂
21 emission inventory derived using a point source database and satellite observations of
22 nighttime lights, *Atmos. Chem. Phys.*, 11, 543–556, doi:10.5194/acp-11-543-2011, 2011.
- 23 Onogi, K., Tsutsui, J., Koide, H., Sakamoto, M., Kobayashi, S., Hatsushika, H., Matsumoto, T.,
24 Yamazaki, N., Kamahori, H., Takahashi, K., Kadokura, S., Wada, K., Kato, K., Oyama, R.,
25 Ose, T., Mannoji, N., and Taira, R.: The JRA-25 Reanalysis, *J. Meteor. Soc. Japan*, 85, 369–
26 432, 2007.
- 27 Patra, P. K., Law, R. M., Peters, W., Rodenbeck, C., Takigawa, M., Aulagnier, C., Baker, I.,
28 Bergmann, D. J., Bousquet, P., Brandt, J., Bruhwiler, L., Cameron-Smith, P. J., Christensen,
29 J. H., Delage, F., Denning, A. S., Fan, S., Geels, C., Houweling, S., Imasu, R., Karstens, U.,
30 Kawa, S. R., Kleist, J., Krol, M. C., Lin, S.-J., Lokupitiya, R., Maki, T., Maksyutov, S., Niwa, Y.,
31 Onishi, R., Parazoo, N., Pieterse, G., River, L., Satoh, M., Serrar, S., Taguchi, S., Vautard, R.,
32 Vermeulen, A. T., and Zhu, Z.: TransCom model simulations of hourly atmospheric CO₂:
33 Analysis of synoptic-scale variations for the period 2002–2003, *Global Biogeochem. Cy.*,
34 22, GB4013, doi:10.1029/2007GB003081, 2008.
- 35 Patra, P. K., Houweling, S., Krol, M., Bousquet, P., Belikov, D., Bergmann, D., Bian, H., Cameron-
36 Smith, P., Chipperfield, M. P., Corbin, K., Fortems-Cheiney, A., Fraser, A., Gloor, E., Hess, P.,
37 Ito, A., Kawa, S. R., Law, R. M., Loh, Z., Maksyutov, S., Meng, L., Palmer, P. I., Prinn, R. G.,
38 Rigby, M., Saito, R., and Wilson, C.: TransCom model simulations of CH₄ and related
39 species: linking transport, surface flux and chemical loss with CH₄ variability in the
40 troposphere and lower stratosphere, *Atmos. Chem. Phys.*, 11, 12813–12837,

1 doi:10.5194/acp-11-12813-2011, 2011.

2 Peters, W., Miller, J. B., Whitaker, J., Denning, A. S., Hirsch, A., Krol, M. C., Zupanski, D.,
3 Bruhwiler, L., and Tans, P. P.: An ensemble data assimilation system to estimate CO₂
4 surface fluxes from atmospheric trace gas observations, *J. Geophys. Res.*, 110, D24304,
5 doi:10.1029/2005JD006157, 2005.

6 Peters, W., ~~Jacobson, A. R., Sweeney, C., Andrews, A. E., Conway, T. J., Masarie, K., Miller, J. B.,~~
7 ~~Bruhwiler, L., M. P., Pétron, G., Whitaker, J., Denning, S., Hirsch, A. I., Worthy, D. E. J., van~~
8 ~~der Werf, G. R., Randerson, J. T., Wennberg, P. O., Krol, M. C., Zupanski, D., Bruhwiler, L.,~~
9 and Tans, P. P.: An ensemble data assimilation system to estimate CO₂ surface fluxes
10 from atmospheric trace gas observations, *J. Geophys. Res.*, perspective on North
11 American carbon dioxide exchange: CarbonTracker, *Proc. Nat. Academy Sci.*, 104,
12 18,925–18,930, doi:10.1073/pnas.0708986104, 2007.110, D24304,
13 doi:10.1029/2005JD006157, 2005. Peylin, P., Rayner, P. J., Bousquet, P., Carouge, C., Hourdin,
14 F., Heinrich, P., Ciais, P., and AEROCARB contributors: Daily CO₂ flux estimates over
15 Europe from continuous atmospheric measurements: 1, inverse methodology, *Atmos.*
16 *Chem. Phys.*, 5, 3173–3186, doi:10.5194/acp-5-3173-2005, 2005.

17 Peylin, P., Law, R. M., Gurney, K. R., Chevallier, F., Jacobson, A. R., Maki, T., Niwa, Y., Patra, P. K.,
18 Peters, W., Rayner, P. J., Rödenbeck, C., and Zhang, X.: Global atmospheric carbon budget:
19 results from an ensemble of atmospheric CO₂ inversions, *Biogeosciences Discuss.*, 10,
20 5301–5360, doi:10.5194/bgd-10-5301-2013, 2013.

21 Rayner P. J., and O'Brien, D. M.: The utility of remotely sensed CO₂ concentration data in
22 surface source inversions, *Geophys. Res. Lett.*, 28, 175–178, 2001.

23 Rigby, M., Manning, A. J., and Prinn, R. G.: Inversion of long-lived trace gas emissions using
24 combined Eulerian and Lagrangian chemical transport models, *Atmos. Chem. Phys.*, 11,
25 9887–9898, doi:10.5194/acp-11-9887-2011, 2011.

26 Rodgers, C. D.: Inverse methods for atmospheric sounding, vol. 2 of Series on Atmospheric,
27 Oceanic and Planetary Physics, World Scientific, Singapore, 2000.

28 Rödenbeck, C., Houweling, S., Gloor, M., and Heimann, M.: Time-dependent CO₂ flux history
29 1982–2001 inferred from atmospheric CO₂ inversions based on interannually varying
30 tracer data using a global inversion of atmospheric transport, *Tellus B*, 55, 488–
31 497 *Atmos. Chem. Phys.*, 3, 1919–1964, doi:10.5194/acp-3-1919-2003, 2003.

32 Rödenbeck, C., Gerbig, C., Trusilova, K., and Heimann, M.: A two-step scheme for high-
33 resolution regional atmospheric trace gas inversions based on independent models,
34 *Atmos. Chem. Phys.*, 9, 5331–5342, doi:10.5194/acp-9-5331-2009, 2009.

35 Saito, M., Ito, A., and Maksyutov, S.: Evaluation of biases in JRA-25/JCDAS precipitation and
36 their impact on the global terrestrial carbon balance, *J. Climate*, 24, 4109–4125, 2011.

37 Saito, M., Ito, A., and Maksyutov, S.: Optimization of a prognostic biosphere model in
38 atmospheric CO₂ variability and terrestrial biomass, *Geosci. Model Dev. Discuss.*, 6,
39 4243–4280, doi:10.5194/gmdd-6-4243-2013, 2013.

- 1 Saeki, T., Maksyutov, S., Sasakawa, M., Machida, T., Arshinov, M., Tans, P., Conway, T. J., Saito,
2 M., Valsala, V., Oda, T., Andres, R. J., and Belikov, D.: Carbon flux estimation for Siberia by
3 inverse modeling constrained by aircraft and tower CO₂ measurements, *J. Geophys. Res.*
4 *Atmos.*, 118, doi:10.1002/jgrd.50127, 2013.
- 5 Sasakawa, M., K. Shimoyama, T. Machida, N. Tsuda, H. Suto, M. Arshinov, D. Davydov, A.
6 Fofonov, O. Krasnov, T. Saeki, Y. Koyama, and S. Maksyutov, Continuous measurements
7 of methane from a tower network over Siberia, *Tellus* 62B, 403–416, 2010.
- 8 Stohl, A., Forster, C., Frank, A., Seibert, P., and Wotawa, G.: Technical note: The Lagrangian
9 particle dispersion model FLEXPART version 6.2, *Atmos. Chem. Phys.*, 5, 2461–2474,
10 doi:10.5194/acp-5-2461-2005, 2005.
- 11 Stohl, A., Seibert, P., Arduini, J., Eckhardt, S., Fraser, P., Grealley, B. R., Lunder, C., Maione, M.,
12 Mhle, J., O'Doherty, S., Prinn, R. G., Reimann, S., Saito, T., Schmidbauer, N., Simmonds, P.
13 G., Vollmer, M. K., Weiss, R. F., and Yokouchi, Y.: An analytical inversion method for
14 determining regional and global emissions of greenhouse gases: Sensitivity studies and
15 application to halocarbons, *Atmos. Chem. Phys.*, 9, 1597–1620, doi:10.5194/acp-9-1597-
16 2009, 2009.
- 17 Takagi, H., Saeki, T., Oda, T., Saito, M., Valsala, V., Belikov, D., Saito, R., Yoshida, Y., Morino, I.,
18 Uchino, O., Andres, R. J., Yokota, T., and Maksyutov, S.: On the benefit of GOSAT
19 observations to the estimation of regional CO₂ fluxes, *SOLA*, 7, 161–164, 2011.
- 20 Tans, P. P., Conway, T. J., and Nakazawa, T.: Latitudinal distribution of the sources and sinks of
21 atmospheric carbon dioxide derived from surface observations and an atmospheric
22 transport model, *J. Geophys. Res.*, 94, 5151–5172, 1989.
- 23 Tarantola, A.: *Inverse Problem Theory and Methods for Model Parameter Estimation*, Society
24 for Industrial and Applied Mathematics, Philadelphia, USA, 2005.
- 25 Thompson, R. L., and Stohl, A.: FLEXINVERT: an atmospheric Bayesian inversion framework
26 for determining surface fluxes of trace species using an optimized grid, *Geosci. Model*
27 *Dev.*, 7, 2223–2242, doi:10.5194/gmd-7-2223-2014, 2014.
- 28 ~~Valsala, V., and Maksyutov, S.: Interannual variability of the air-sea CO₂ flux in the north~~
29 ~~Indian Ocean, *Ocean Dynam.*, 63, 165–178, doi:10.1007/s10236-012-0588-7, 2013.~~
- 30 ~~Tohjima, Y., Terao, Y., Mukai, H., Machida, T., Nojiri, Y., & Maksyutov, S.: ENSO-related~~
31 ~~variability in latitudinal distribution of annual mean atmospheric potential oxygen~~
32 ~~(APO) in the equatorial Western Pacific. *Tellus B*, 67,~~
33 ~~doi:http://dx.doi.org/10.3402/tellusb.v67.25869, 2015.~~
- 34 ~~Valsala V. and Maksyutov S.: Simulation and assimilation of global ocean pCO₂ and air-sea CO₂~~
35 ~~fluxes using ship observations of surface ocean pCO₂ in a simplified biogeochemical~~
36 ~~offline model, *Tellus-B*, 62B, 821–840, doi:10.1111/j.1600-0889.2010.00495.x, 2010.~~
- 37 van der Werf, G. R., Randerson, J. T., Giglio, L., Collatz, G. J., Mu, M., Kasibhatla, P. S., Morton, D.
38 C., DeFries, R. S., Jin, Y., and van Leeuwen, T. T.: Global fire emissions and the
39 contribution of deforestation, savanna, forest, agricultural, and peat fires (1997–2009),

- 1 Atmos. Chem. Phys., 10, 11707–11735, doi:10.5194/acp-10-11707-2010, 2010.
- 2 Wilson, C., Chipperfield, M. P., Gloor, M., and Chevallier, F.: Development of a variational flux
3 inversion system (INVICAT v1.0) using the TOMCAT chemical transport model, Geosci.
4 Model Dev., 7, 2485–2500, doi:10.5194/gmd-7-2485-2014, 2014.
- 5 | [WDCGG: WMO World Data Centre for Greenhouse Gases, Japan Meteorological Agency, Tokyo,](http://ds.data.jma.go.jp/gmd/wdcgg/introduction.html)
6 | [available at: http://ds.data.jma.go.jp/gmd/wdcgg/introduction.html, 2015.](http://ds.data.jma.go.jp/gmd/wdcgg/introduction.html)
- 7 Yokota, T., Yoshida, Y., Eguchi, N., Ota, Y., Tanaka, T., Watanabe, H., and Maksyutov, S.: Global
8 concentrations of CO₂ and CH₄ retrieved from GOSAT: First preliminary results, SOLA, 5,
9 160–163, doi:10.2151/sola.2009-041, 2009.
- 10

1 **Table 1.** The coupled model setups analyzed in this study.

Case	Resolution, °		Flux combination
	NIES TM	FLEXPART	
Cs-1	10.0	1.0	VISIT + CDIAC + OTTM
Cs-2	2.50	1.0	VISIT + CDIAC + OTTM
Cs-3	1.25	1.0	VISIT + CDIAC + OTTM

2

3

Table 2. WDCGG continuous observation sites.

#	<u>Identifying code</u>	<u>Location</u>	<u>Lat., °</u>	<u>Lon., °</u>	<u>Height, m</u>	<u>Contributor, contact person</u>
<u>1</u>	<u>ALT</u>	<u>Alert, Canada</u>	<u>82.45</u>	<u>-62.52</u>	<u>210</u>	<u>EC, Doug Worthy</u>
<u>2</u>	<u>AMS</u>	<u>Amsterdam Island, France</u>	<u>-37.8</u>	<u>77.53</u>	<u>55</u>	<u>LSCE, Michel Ramonet</u>
<u>3</u>	<u>AMY</u>	<u>Anmyeon-do, Korea</u>	<u>36.53</u>	<u>126.32</u>	<u>47</u>	<u>KMA, Ms. Haeyoung Lee</u>
<u>4</u>	<u>BRW</u>	<u>Barrow, USA</u>	<u>71.32</u>	<u>-156.6</u>	<u>11</u>	<u>NOAA/ESRL, Kirk W Thoning</u>
<u>5</u>	<u>CMN</u>	<u>Monte Cimone, Italy</u>	<u>44.18</u>	<u>10.7</u>	<u>2165</u>	<u>IAFMS, Centro Aeronautica Militare di Montagna</u>
<u>6</u>	<u>CPT</u>	<u>Cape Point, South Africa</u>	<u>-34.35</u>	<u>18.48</u>	<u>230</u>	<u>SAWS, Thumeka Mkololo</u>
<u>7</u>	<u>HUN</u>	<u>Hegyhatsal, Hungary</u>	<u>46.95</u>	<u>16.65</u>	<u>248</u>	<u>HMS, Laszlo Haszpra</u>
<u>8</u>	<u>IZO</u>	<u>Izana, Spain</u>	<u>28.3</u>	<u>-16.5</u>	<u>2367</u>	<u>AEMET, Angel J. Gomez-Pelaez</u>
<u>9</u>	<u>JBN</u>	<u>Jubany, Argentina</u>	<u>-62.23</u>	<u>-58.67</u>	<u>15</u>	<u>CNR-ICES, DNA-IAA, Claudio Rafanelli</u>
<u>10</u>	<u>MHD</u>	<u>Mace Head, Ireland</u>	<u>53.33</u>	<u>-9.9</u>	<u>8</u>	<u>LSCE, Michel Ramonet</u>
<u>11</u>	<u>MLO</u>	<u>Mauna Loa, USA</u>	<u>19.54</u>	<u>-155.58</u>	<u>3397</u>	<u>NOAA/ESRL, Kirk W Thoning</u>
<u>12</u>	<u>MNM</u>	<u>Minamitorishima, Japan</u>	<u>24.28</u>	<u>153.98</u>	<u>8</u>	<u>JMA, Greenhouse Gas observation section</u>
<u>13</u>	<u>PAL</u>	<u>Pallas-Sammaltunturi, Finland</u>	<u>67.97</u>	<u>24.12</u>	<u>560</u>	<u>FMI, Juha Hatakka</u>
<u>14</u>	<u>PRS</u>	<u>Plateau Rosa, Italy</u>	<u>45.93</u>	<u>7.7</u>	<u>3480</u>	<u>RSE, Francesco Apadula</u>
<u>15</u>	<u>PUY</u>	<u>Puy de Dome, France</u>	<u>45.77</u>	<u>2.97</u>	<u>1465</u>	<u>LSCE, Michel Ramonet</u>
<u>16</u>	<u>SSL</u>	<u>Schauinsland, Germany</u>	<u>47.92</u>	<u>7.92</u>	<u>1205</u>	<u>UBA, Karin Uhse</u>
<u>17</u>	<u>WSA</u>	<u>Sable Island, Canada</u>	<u>43.93</u>	<u>-60.02</u>	<u>5</u>	<u>EC, Doug Worthy</u>
<u>18</u>	<u>YON</u>	<u>Yonagunijima, Japan</u>	<u>24.47</u>	<u>123.02</u>	<u>30</u>	<u>JMA, Greenhouse Gas observation section</u>

<u>19</u>	<u>ZEP</u>	<u>Zeppelifjellet,</u> Norway	<u>78.9</u>	<u>11.88</u>	<u>475</u>	<u>ITM,</u> Birgitta Noone
-----------	------------	----------------------------------	-------------	--------------	------------	-------------------------------

1

2 Here AEMET - Izana Atmospheric Research Center, Meteorological State Agency of Spain;

3 CNR-ICES - International Center for Earth Sciences - CNR, Institute of Acoustics and Sensors;

4 DNA-IAA - Direccion Nacional del Antartico- Istituto Antartico Argentino; EC - Environment

5 Canada; HMS - Hungarian Meteorological Service; IAFMS - Italian Air Force Meteorological

6 Service; ITM - Department of Applied Environmental Science, Stockholm University; JMA -

7 Japan Meteorological Agency; KMA - Korea Meteorological Administration; LSCE - Laboratoire

8 des Sciences du Climat et de l'Environnement; NOAA/ESRL - National Oceanic and

9 Atmospheric Administration/Earth System Research Laboratory; RSE - Ricerca sul Sistema

10 Energetico - RSE S.p.A.; FMI - Finnish Meteorological Institute; SAWS - South African Weather

11 Service; UBA - Federal Environmental Agency Germany.

12

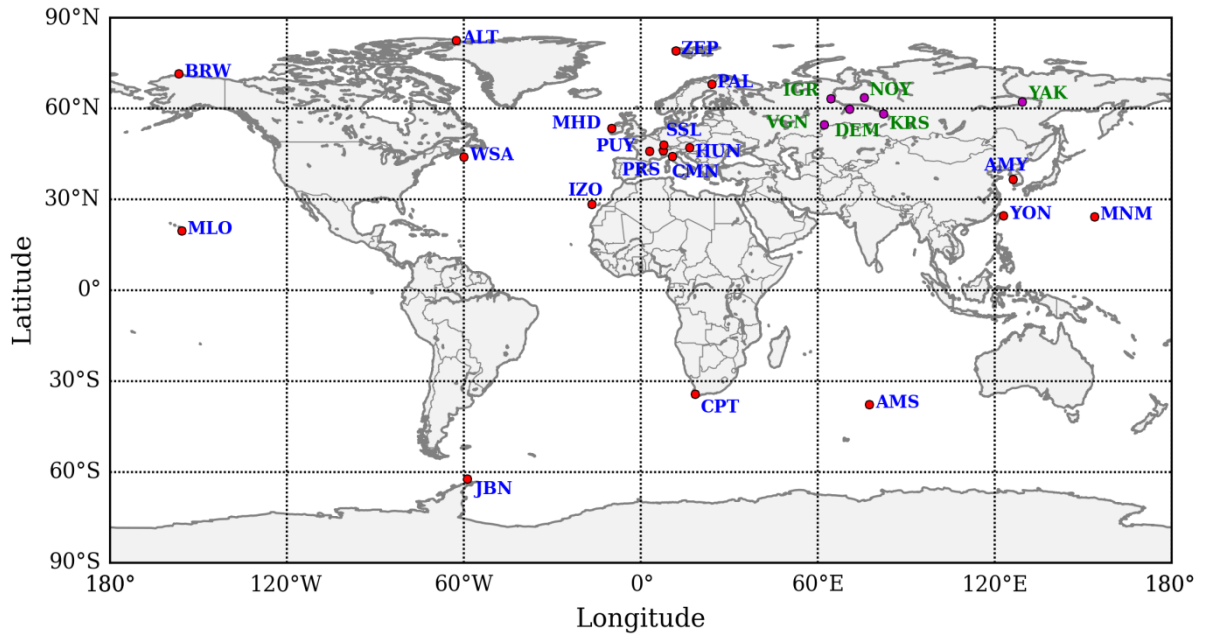
1

Table 2, Table 3. Tower network sites in Siberia (JR-STATION).

#	Identifying code	Location	Latitude Lat. / °	Longitude Lon / °	Sampling height (m)Height / m
1	DEM	Demyanskoe	59°47'29".79	70°52'16".87	63
2	IGR	Igrim	63°11'25".19	64°24'56".42	47
3	KRS	Karasevoe	58°14'44".25	82°25'28".42	67
4	NOY	Noyabrsk	63°25'45".43	75°46'48".78	43
	SVV	Savvushka	51°19'30"	82°07'40"	52
5	VGN	Vaganovo	54°29'50".50	62°19'29".32	85
6	YAK	Yakutsk	62°05'19".09	129°21'21".3 6	77

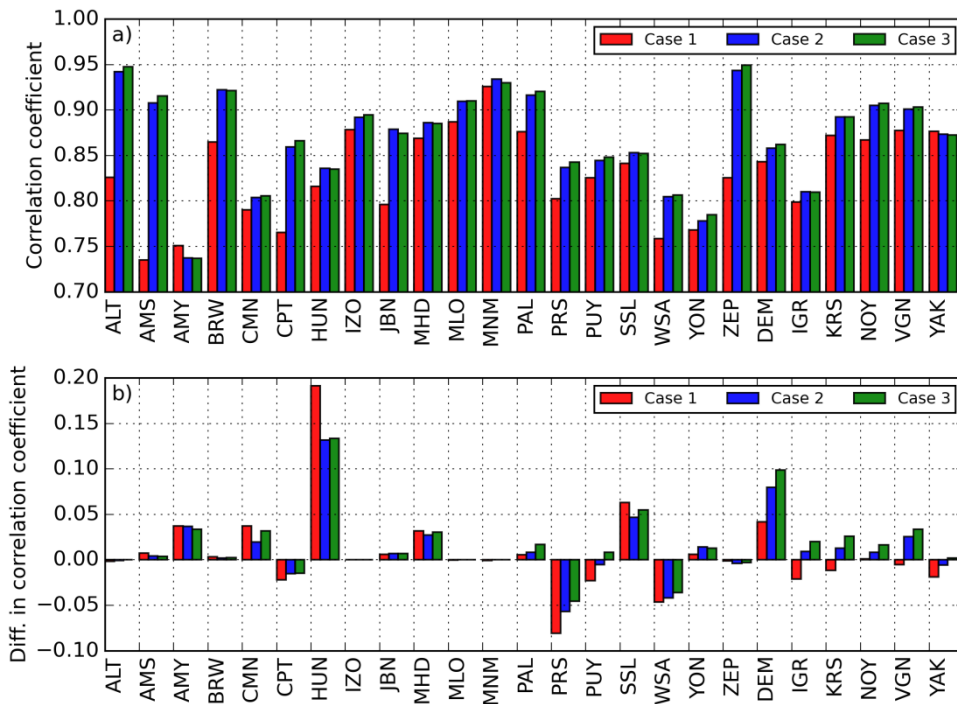
2

3 | ~~Information on~~



1
2
3
4
5

Fig. 1. Map showing the location of the 19 WDCGG sites (red dots, blue labels) and 6 tower network sites in Siberia (magenta dots, green labels) for which we have performed comparison using forward GELCA simulation.

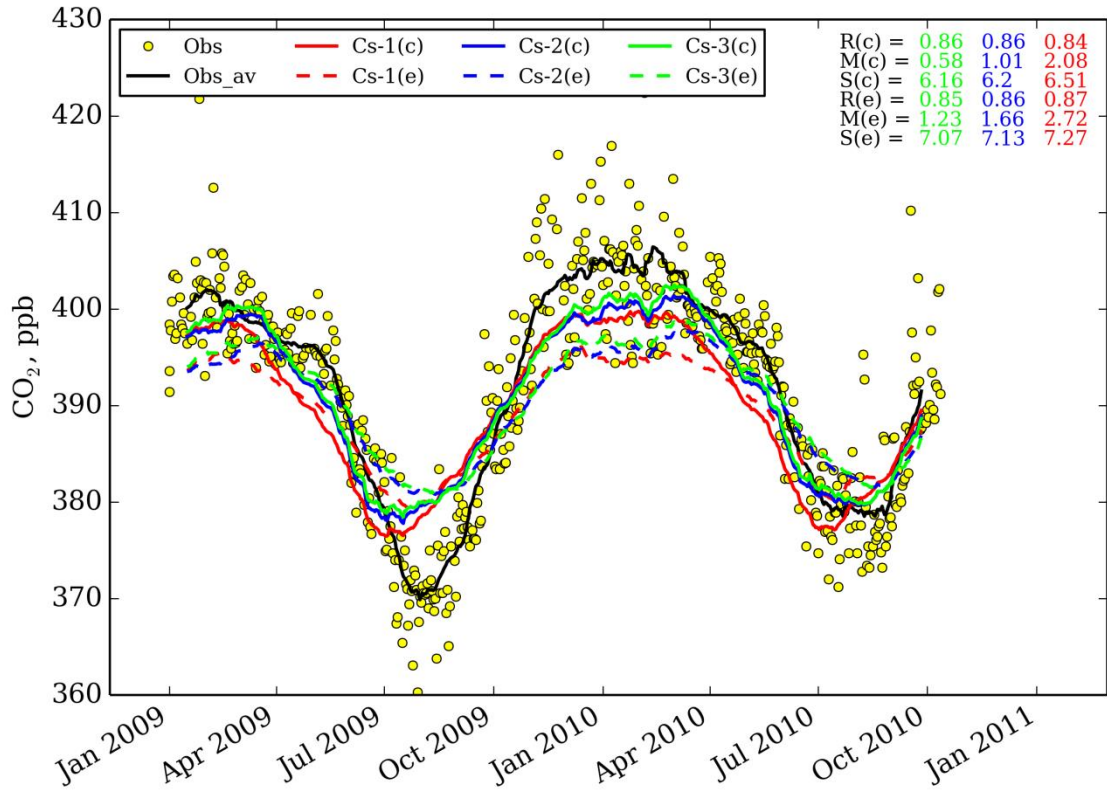


6

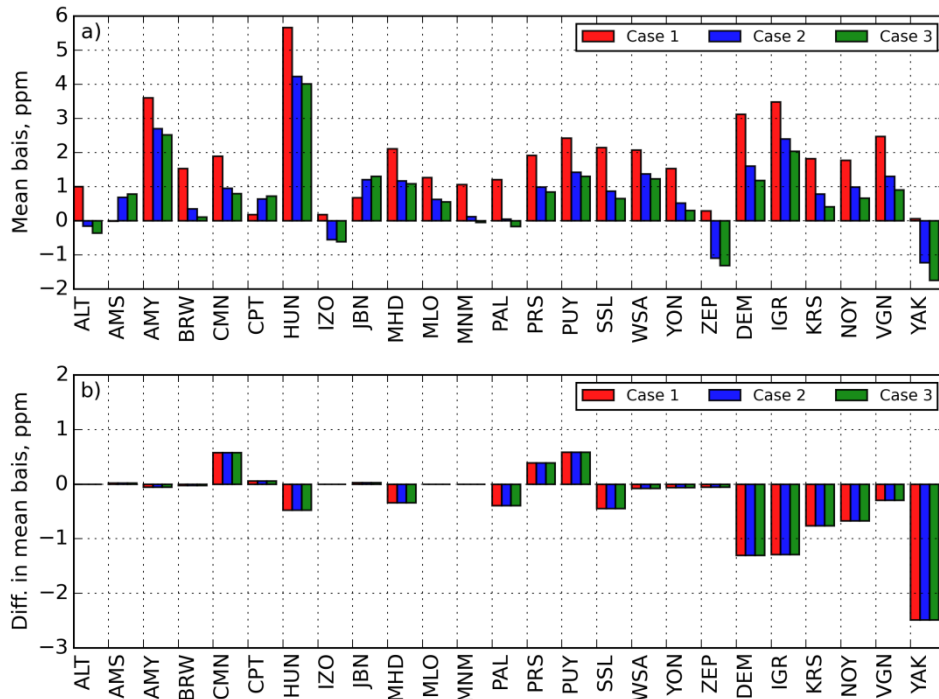
1 **Table 3.** **Fig. 2.** a) Correlation coefficients between the CO₂ concentrations simulated with the
 2 coupled model and those observed, b) difference in correlation coefficients, mean bias,
 3 and standard deviations between simulations using the coupled (due to the
 4 application of the Lagrangian component (positive values mean the results of the
 5 coupled model are better than those of the Eulerian model alone) model and
 6 observations. at the selected WDCGG and JR-STATION locations for 2009-2010.

Site	# of obs.	Cs-1			Cs-2			Cs-3		
		Correlation coefficient	Mean bias, ppm	STD, ppm	Correlation coefficient	Mean bias, ppm	STD, ppm	Correlation coefficient	Mean bias, ppm	STD, ppm
DEM	304	0.85 (0.85)	2.92 (3.68)	4.19 (4.37)	0.86 (0.84)	1.27 (2.03)	4.01 (4.37)	0.87 (0.84)	0.69 (1.45)	4.02 (4.27)
IGR	576	0.84 (0.87)	2.08 (2.72)	6.51 (7.27)	0.86 (0.86)	1.01 (1.66)	6.2 (7.13)	0.86 (0.85)	0.58 (1.23)	6.16 (7.07)
KRS	509	0.88 (0.9)	1.04 (1.44)	5.57 (6.66)	0.90 (0.91)	-0.05 (0.36)	4.92 (5.95)	0.91 (0.91)	-0.63 (0.23)	4.79 (5.79)
NOY	382	0.86 (0.87)	1.48 (2.04)	5.24 (5.72)	0.90 (0.9)	0.07 (0.63)	4.51 (5.08)	0.91 (0.91)	-0.45 (0.12)	4.37 (4.9)
SVV	394	0.89 (0.88)	0.44 (0.16)	6.56 (7.62)	0.91 (0.88)	0.34 (0.06)	5.72 (6.74)	0.90 (0.88)	0.01 (0.27)	5.6 (6.6)
VGN	609	0.88 (0.9)	1.49 (1.69)	5.04 (5.74)	0.91 (0.9)	0.62 (0.82)	4.36 (5.13)	0.91 (0.9)	0.25 (0.45)	4.23 (5.01)
YAK	405	0.84 (0.87)	1.22 (2.44)	5.37 (5.12)	0.86 (0.87)	-0.28 (0.94)	5.68 (4.64)	0.85 (0.86)	-0.81 (0.42)	5.95 (4.74)
Average		0.86 (0.88)	1.52 (2.02)	5.50 (6.07)	0.89 (0.88)	0.43 (0.93)	5.06 (5.58)	0.89 (0.88)	-0.05 (0.45)	5.02 (5.48)

7



1
2
3



4

1
2
3
4
5
6

Fig. 3. a) Mean bias for the CO₂ concentrations simulated with the coupled model, b) difference in mean bias due to the application of the Lagrangian component (for positive bias – the most usual case – negative values mean the results of the coupled model are better than those of the Eulerian model alone) at the selected WDCGG and JR-STATION locations for 2009-2010.

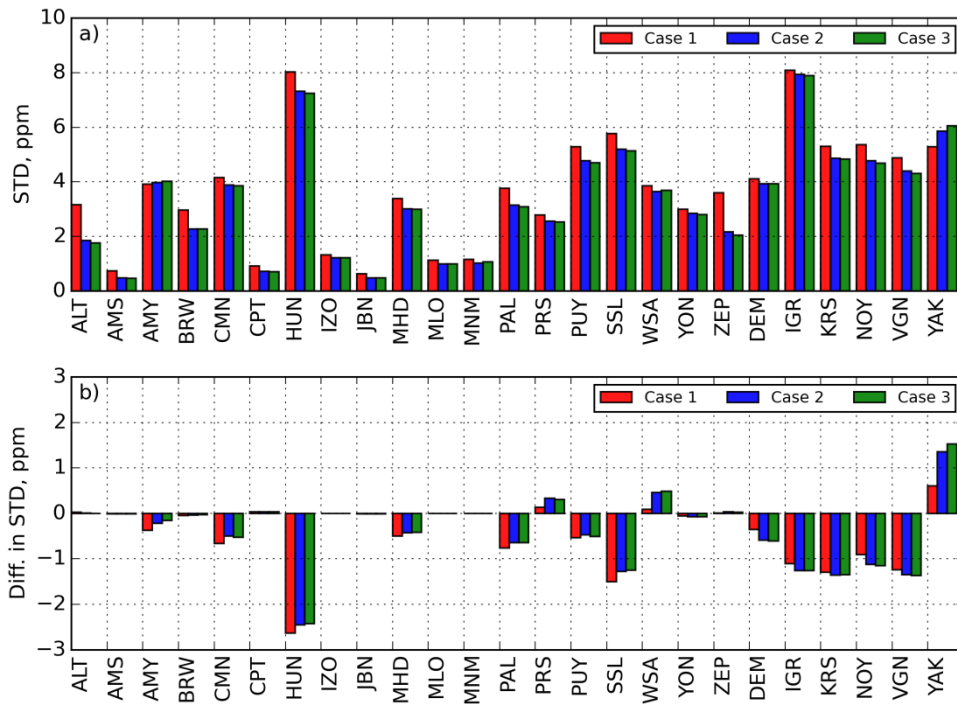
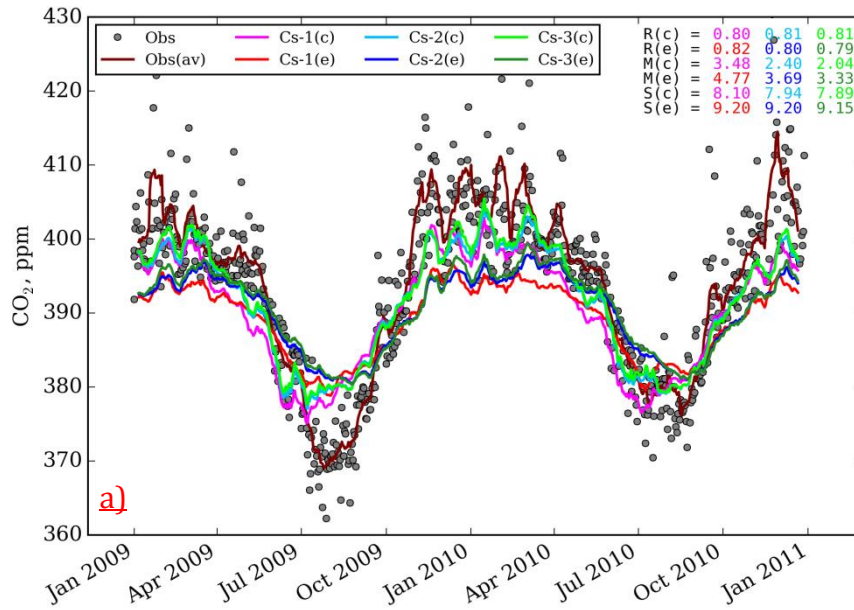
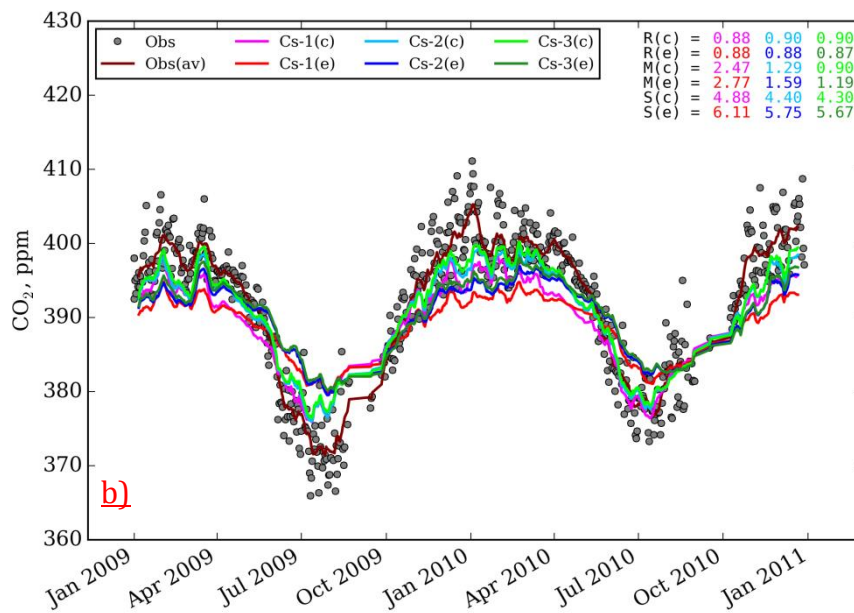


Fig. 4. a) Standard deviation (STD) for the CO₂ concentration model-observation mismatch when using the coupled model, b) difference in STD due to the application of Lagrangian component (negative values mean the results of the coupled model are better than those of the Eulerian model alone) at the selected WDCGG and JR-STATION locations for 2009-2010.

1
2
3
4
5
6
7



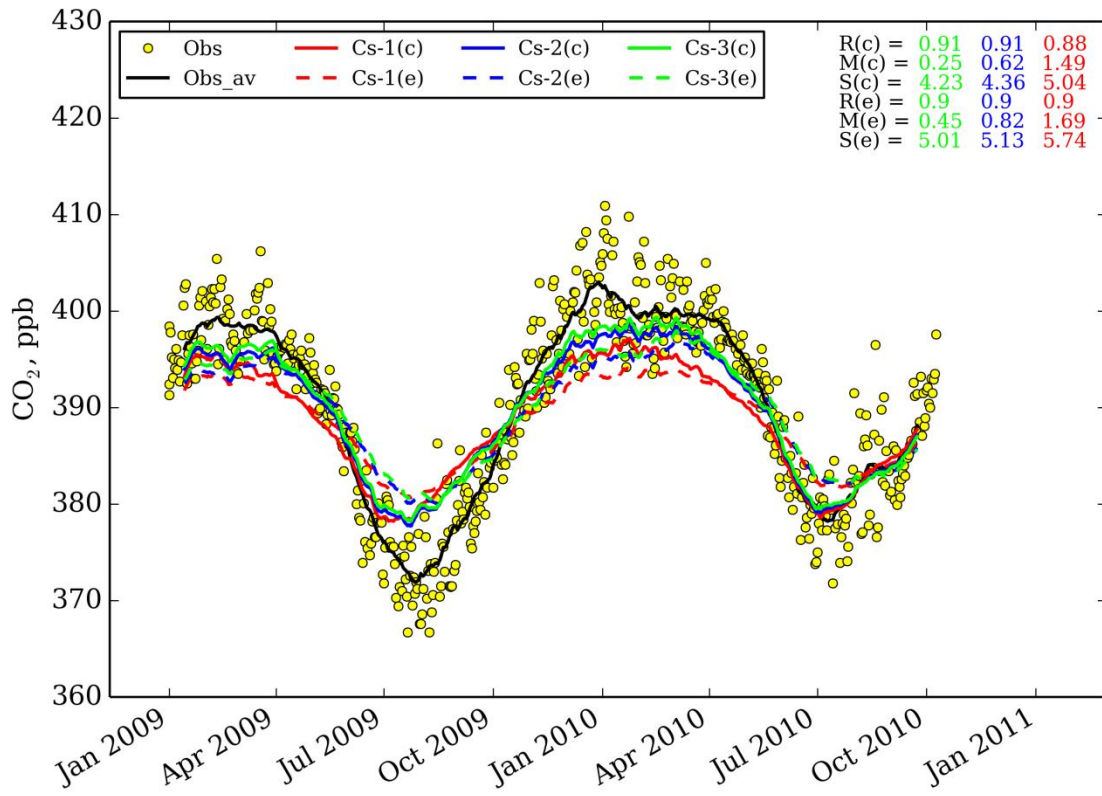
1



2

3 **Fig. 1.** **Fig. 5.** CO₂ mixing ratios observed at **a)** the Igrim tower and **b)** Vaganovo towers, and
 4 simulated using the coupled ("**c**"; **solid line**) and Eulerian-only ("**e**"; **dotted line**)
 5 models using the **model**-setups from Table 1 for 2009–2010. Symbols show individual
 6 observations; lines depict **the moving average-two-week running averages**. Here, **r**, **s**,
 7 **M**, **R**, **S** and **M** mean the Pearson correlation, standard deviation and mean bias
 8 **correspondently respectively**.

9



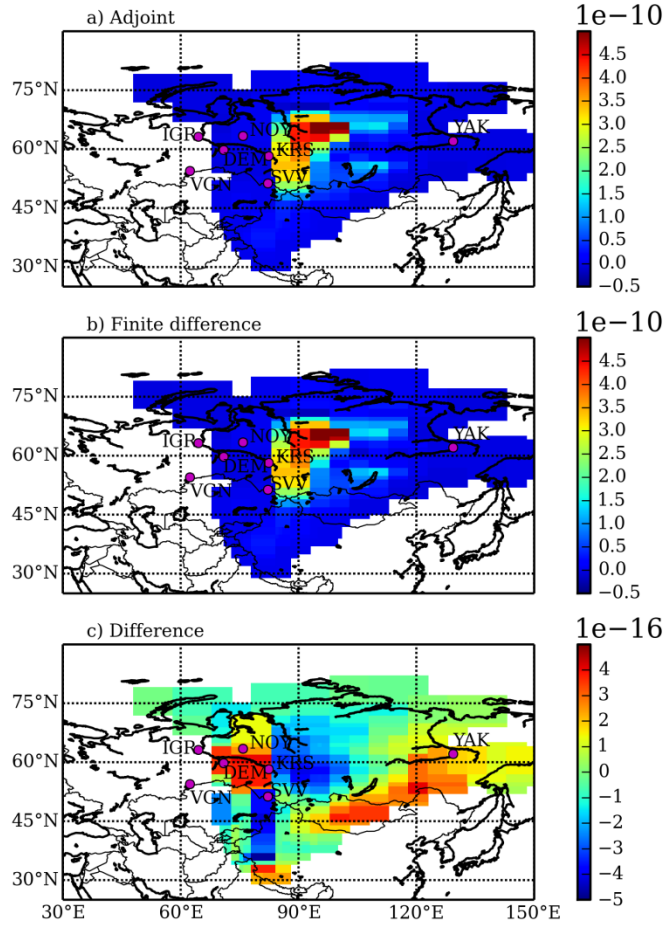
1

2

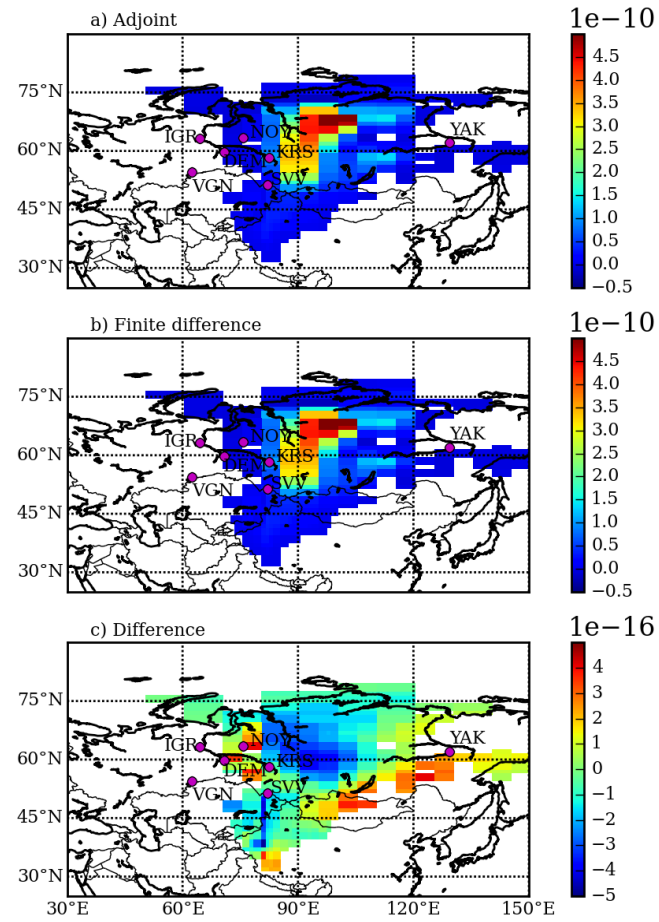
~~Fig. 2. As for Fig 2, but for the Vaganovo tower.~~

3

1

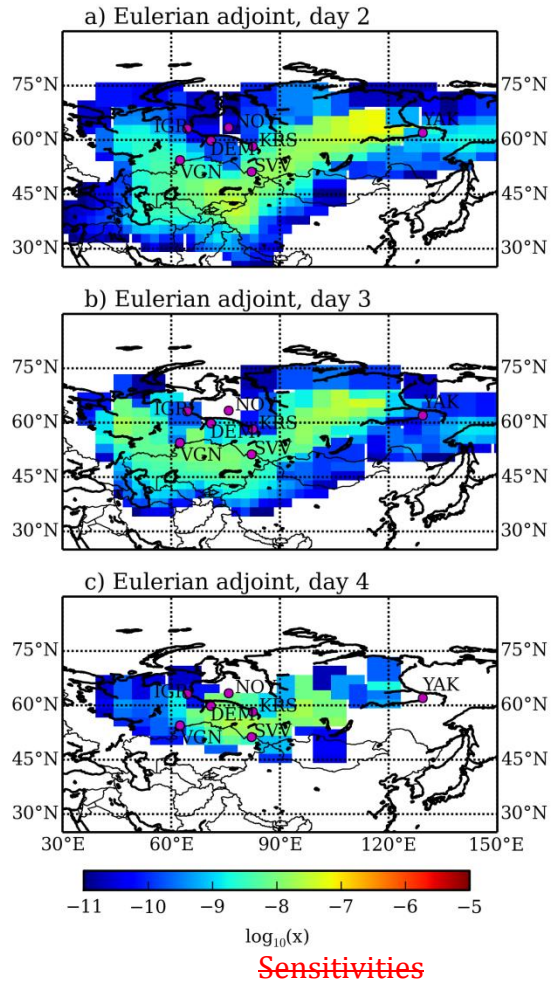


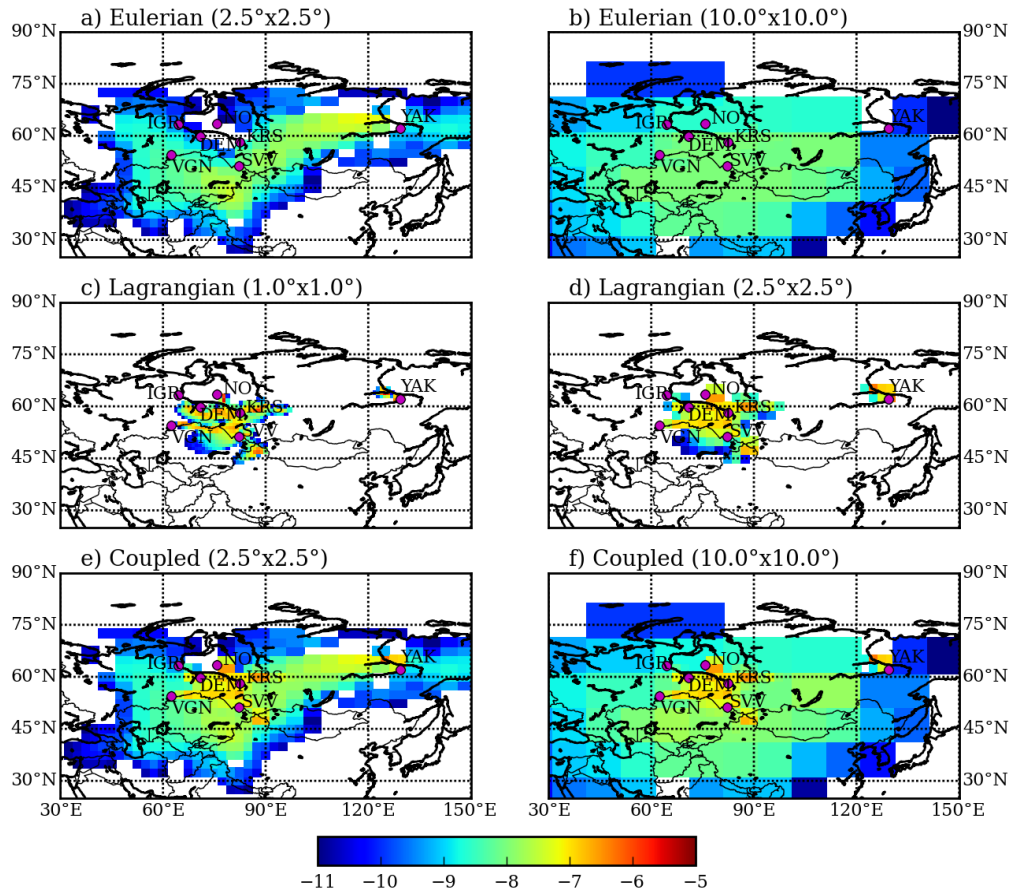
2



1 **Fig. 3.Fig. 6.** Comparison of sensitivities of CO₂ concentrations (ppm/(μ mol/m²s)) for test 1: (a)
2 sensitivity calculated considering only the Eulerian adjoint model at a resolution of
3 2.5°, (b) the same sensitivity calculated directly from NIES forward runs using the one-
4 sided numerical finite difference method with perturbations of ϵ , and c) the relative
5 difference between derived adjoint and the numerical finite difference gradients.
6 Magenta dots with labels depicts the locations and names of the Siberian
7 ~~observations~~observation towers.
8

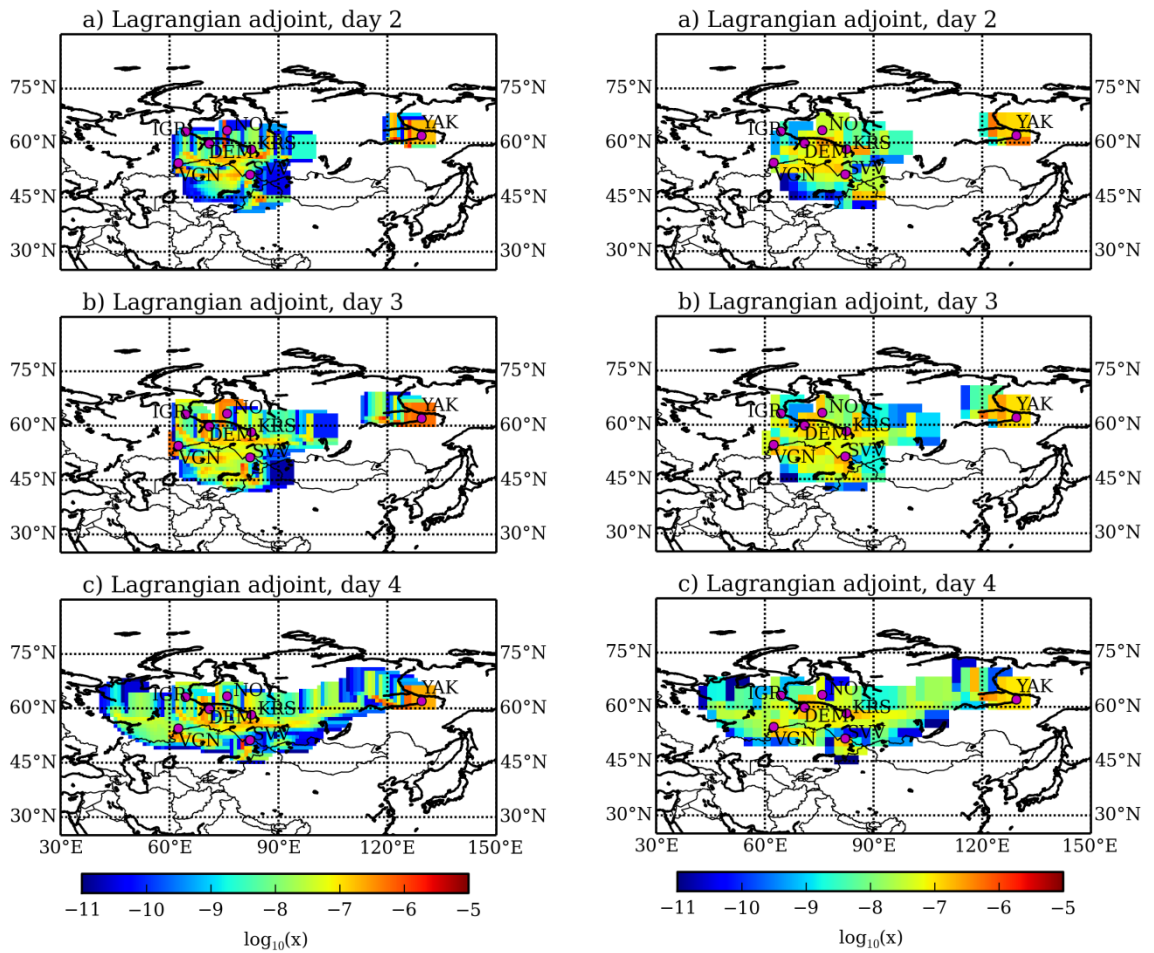
1
2





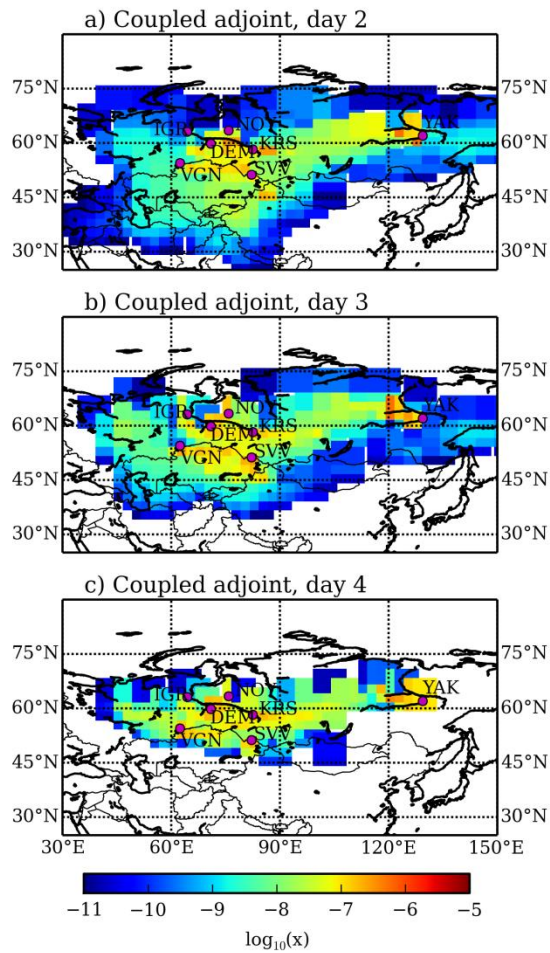
1
2
3
4
5
6

Fig. 4. — Comparison of sensitivities of CO₂ concentrations ($[\text{ppm}/(\mu\text{mol}/\text{m}^2\text{s})]$ with respect to concentrations in adjacent cells, considering only) at day 2 (see Sect. 5.2.2) calculated using: a) the Eulerian adjoint model at with a resolution of 2.5°.



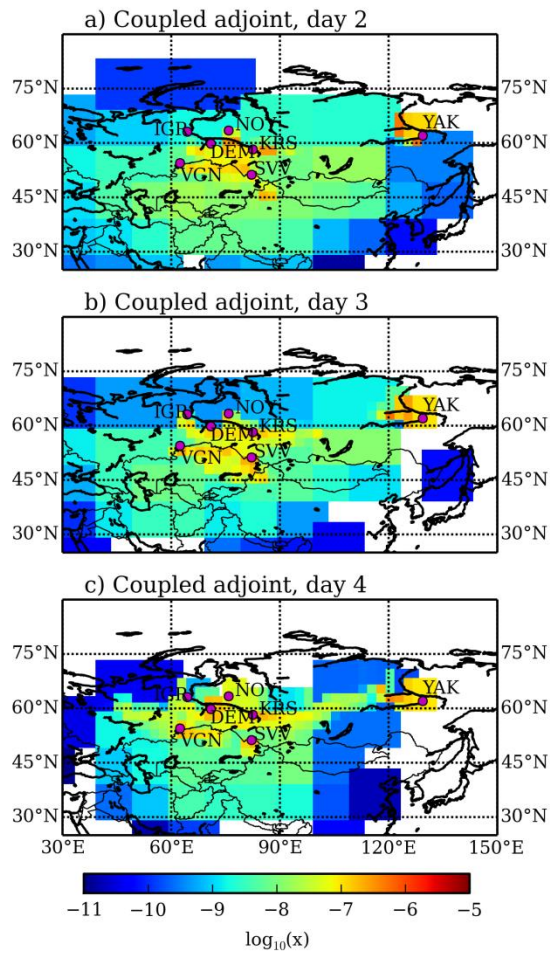
1
2
3
4
5
6

Fig. 5. ~~Same as Fig. 4, but considering only~~, b) the Eulerian adjoint with a resolution of 10.0°, c) the Lagrangian adjoint model. ~~The left panels show results on the native model grid with a resolution of 1.0°, while the right panels show the results~~ d) as for c), but aggregated on the grid atwith a resolution of 2.5°.



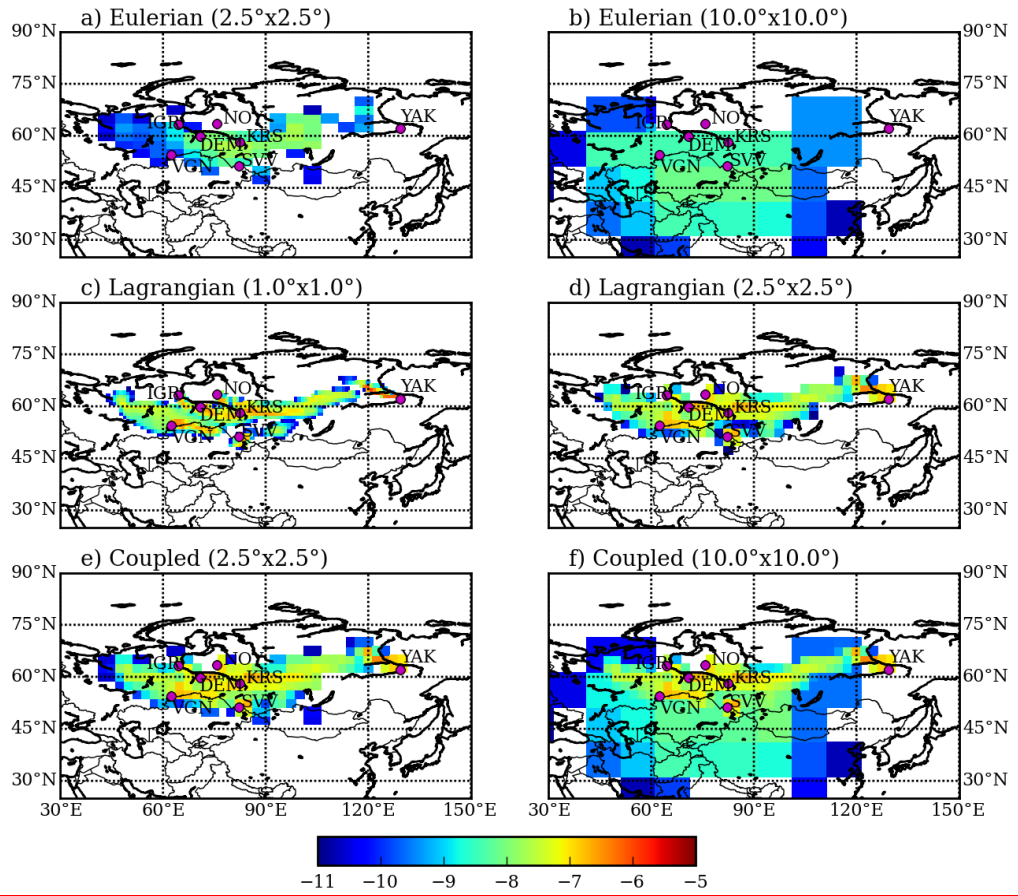
1
2
3
4
5

Fig. 6. Same as Fig.4, but considering ^e the coupled adjoint model. Results; results from the Lagrangian adjoint model were aggregated on the grid of NIES-TM at with a resolution of 2.5°.



1
2
3
4
5

Fig. 7. As, f) as for Fig. 6, e), but results from the resolution of the Eulerian adjoint model were aggregated on was 10.0°. Note the grid at a resolution of 10.0°-logarithmic color scale for the plots.



1
2
3

Fig. 8. As for Fig. 7, but for day 4.